Establishing a Proximity-Ligation Method to Understand the Interactome of Protein Aggregates in Neurodegenerative Diseases

Paulina Szwaja

B.Sc., Macquarie University

Department of Biomedical Sciences

Faculty of Medicine, Health and Human Sciences

Macquarie University, New South Wales, Australia

This thesis is presented to Macquarie University in fulfillment of the Master of Research in Biomedical Sciences

Submitted for examination:

June 2020

Table of Contents

Statement of Originality

This work has not previously been submitted for a degree or diploma in any university. To the best of my knowledge and belief, the thesis contains no material previously published or written by another person except where due reference is made in the thesis itself.

(Signed)_____ _____   Date: 10th June 2020

Paulina Szwaja

Ethics and Biosafety approvals

The human postmortem tissue from PSP patients used in this project was provided through collaboration with Dr Dean Pountney, Griffith University (MSC/16/11/HREC). To use the tissue at Macquarie University, the HREC at Griffith University approved use under MQ HREC permit held by the Macquarie University Neurodegenerative Disease Biobank (5201600387). The use of this postmortem tissue was also covered under an Institutional Biosafety Permit held by the Neurodegenerative Disease Biobank's (5201700825).

This project used patient-derived fibroblasts that were collected and maintained through the Macquarie University Disease Biobank. This project used these fibroblasts for cell culture experiments, as approved under MQ HREC permit held by the Macquarie University Disease Biobank (5201600387). The use of these cells was also covered under an Institutional Biosafety Permit held by the Neurodegenerative Disease Biobank (5201700825).

COVID-19 disruption to research project

This project was disrupted by the unfortunate circumstances associated with the global COVID-19 pandemic. This placed some restrictions upon laboratory-based activities towards the end of this project, including delays to mass spectrometry access (for proteomic analysis) and PC2 lab access for biochemical and immunohistochemical validation of proteins-of-interest. All efforts were made to overcome these disruptions, with the impact described where appropriate in this thesis.

Paulina Szwaja (candidate)

Professor Roger Chung (primary supervisor)

Contributors

Name	Specific Contribution
Paulina Szwaja (PS)	Write up of thesis and manuscripts for publication; optimized biotin cleavage and DAPI staining protocols; experiments primarily undertaken by PS with the supervision, training and guidance of SR and RR; imaged HEK293 cells shown in chapter 2; labelled 4 PSP sections used for this project; primarily analysed data.
Stephanie Rayner (SR)	Trained and assisted PS with experiments – primarily guided culturing cells and protocol optimization; assisted with preparing samples for mass spectrometry analysis; guided PS on Proteome Discoverer 2.4 and Ingenuity Pathway Analysis software.
Rowan Radford (RR)	Optimized BAR technique for PSP tissue used in this project; imaged all tissue and most cell figures that appear in this thesis; trained and supervized PS with BAR labelling of PSP tissue; labelled 12 PSP sections used for this project.
Albert Lee (AL)	Trained PS on Ingenuity Pathway Analysis software and provided intellectual guidance in the data analysis process.
Flora Cheng (FC)	Ran all samples through the mass spectrometer and uploaded files to Proteome Discoverer 2.4.
Jennifer Rowland (JR)	Provided intellectual guidance for thesis write-up.
Roger Chung (RC)	Oversaw the project, assisted with some figure creations, and provided intellectual guidance throughout.

Acknowledgments

I would like express my gratitude to Prof. Roger Chung for welcoming me into his lab and providing me the opportunity to work on such an interesting project. Despite your endless work commitments, you have always gone out of your way to help me whenever I needed it and I cannot thank you enough for that. I would also like to thank Rowan Radford and Stephanie Rayner, who ran the project and taught me all I know. Your support, mentorship and immense patience are invaluable and I want you to know I appreciated it the whole way through. Albert Lee, thank you for helping me understand the ins and outs of data analysis, sifting through the insurmountable data proteomics offers. Your advice grounded my approach and led me to complete this project, and complete it well.

I feel so lucky and grateful for all the supportive and patient people in my team, guiding me each step of the way despite their myriad of commitments. You made this past year that much more enjoyable, the obstacles became less intimidating, and I feel ready to tackle the bigger projects in the near future. I cannot imagine a better group of people to take on this experience with.

Jen Rowland, I want to express my thanks for your openness to help with any concerns I had. Your help has led me to become a better all-around science communicator and believer in myself through one of the most challenging yet fulfilling years of my life.

An honourable mention of thanks to my friends and family for always being there for me and continuously supporting my dreams. You have provided me strength during the most challenging of times and I am extremely glad I am surrounded by the best of the best, because you help me see anything is possible with a little push.

List of Abbreviations

ALS = Amyotrophic lateral sclerosis

AR = Abundance ratio

BAR = Biotinylation by antibody recognition

HEK293 = Human embryonic kidney 293

IPA = Ingenuity pathway analysis

MS = Mass spectrometry

p-Tau – Phosphorylated protein tau

POI = Protein of interest

PPI = Protein-protein interaction

PSP = Progressive supranuclear palsy

SA = Sodium arsenite

TDP-43 = Transactive response DNAbinding protein 43kDa

Veh = Vehicle

WT = Wild type

Abstract

Progressive supranuclear palsy (PSP) and amyotrophic lateral sclerosis (ALS) are progressive neurodegenerative diseases pathologically characterized by insoluble inclusions of phosphorylated-Tau (p-Tau) and TDP-43 in neurons respectively. Understanding the protein interactome of these inclusions may uncover important insight into the pathological mechanisms of these diseases. Traditional biochemical extraction methods have several limitations for isolation of detergent-insoluble proteins, with significant sample loss and non-specific binding. Thus to limit these problems, an unbiased proteomic approach was taken that enables labeling of insoluble proteins *in situ* prior to tissue homogenization. This enables targeting of all proteins within a small radius of the protein (inclusion) of interest. This approach, termed biotinylation by antibody recognition (BAR), is a recently described method that will be used in this project to label co-aggregating proteins within post-mortem PSP tissue and fibroblasts from ALS patients. BAR makes use of a primary antibody binding to the protein of interest (POI) to selectively biotinylate proteins in direct proximity to the POI. A secondary antibody conjugated to horseradish peroxidase (HRP) is attached to the primary antibody and the HRP, with the addition of hydrogen peroxide and biotin tyramide, facilitates biotinylation of proteins proximal to the POI. Then the proteins are biochemically isolated and identified using mass spectrometry. With this workflow and bioinformatic analysis, several proteins known to interact with p-Tau and TDP-43 directly and indirectly have been identified along with potentially novel interactors. The data here substantiates this unbiased approach of rapidly labeling and identifying components of aggregates within fixed tissue and cultured cells with a broad application to other diseases and interaction studies.

CHAPTER 1   Introduction, overview and aims

1 Introduction

1.1 Brief project overview

A common characteristic of adult-onset neurodegenerative diseases is the pathological presence of insoluble protein aggregates [16]. The specific distribution and composition of these aggregates has been the basis for the original identification and definition of such diseases, including Alzheimer's disease, Parkinson's disease, and motor neuron diseases [such as amyotrophic lateral sclerosis (ALS)]. This was originally performed based upon post-mortem histopathological characterization of these insoluble protein aggregates, and complemented over the past 20 years by biochemical extraction of protein aggregates to gain deeper understanding of the entire protein composition of the aggregates [37]. The goal of this Master of Research project is to establish a new experimental technique, which uses a proximity-ligation based approach [3] to allow *in situ* proteomic profiling of specific protein aggregates, to reveal new insight into their origin and molecular composition. To validate this technique, it will be used to study protein aggregates in two diseases – progressive supranuclear palsy (PSP) and ALS, which are characterized by aggregation of p-Tau and TDP-43 proteins respectively. This review will briefly describe the key features of pathological protein aggregates in ALS and PSP, and describe the experimental workflow that will be used in this project to proteomically characterize p-Tau and TDP-43 aggregates.

1.2 Tau and Tau-opathies

Tau is a protein encoded by the gene "microtubule associated protein tau" (*MAPT*) and is mainly expressed in the central nervous system neurons [2]. Its main functions are microtubule stabilization, axonal transport facilitation and signal transduction. Alterations in tau lead to many neurodegenerative diseases; this can be at the levels of DNA (*MAPT* mutation), mRNA (altered alternative splicing) and protein (aggregation due to abnormal phosphorylation or cleavage) [49]. Neurodegenerative disorders with these tau alterations are termed tau-opathies, of which there are over 20 [2]. These are further grouped into "primary and secondary tauopathies contingent on whether tau is the main contributor to neurodegeneration or if it is associated with other pathologies respectively" [2]. There are around 10 primary tauopathies, one of which is termed progressive supranuclear palsy (PSP). PSP is a primary tauopathy because the pathological hallmark of the disease is the aggregation of hyperphosphorylated tau within neurons in the brain and is not associated with

another pathology [2, 50]. Tau is thought to be the primary, if not the only, driver of the neuropathology in PSP [2, 20]. An example of a secondary tauopathy is Alzheimer's disease (AD), where the primary pathology is extracellular amyloid-ß deposits in the brain, additionally with intraneuronal tau deposits [2, 54].

1.3 Progressive Supranuclear Palsy

Progressive supranuclear palsy is a progressive neurodegenerative disease first described in 1963 by Richardson [44] with clinical features including postural instability, mild dementia, supranuclear palsy, progressive axial rigidity and bulbar palsy. Richardson's colleagues, Olszewski and Steele [44], classified PSP as a nosological syndrome after identifying consistent pathological patterns in the unusual syndrome. Between 3–6 out of every 100,000 people are afflicted with PSP, men being more often affected than women, and clinical signs typically first present themselves from 60 years of age [13, 36]. A patient with PSP is disabled within 3–5 years of diagnosis and dies 6–12 years from diagnosis, with the most common cause of death being pneumonia [36]. There is no treatment for PSP, however it can be managed with medications (e.g. levodopa and ropinirole, or antidepressants), and other interventions such as weight walking aids for fall prevention and bifocals or prisms to remedy the difficulty in focusing their gaze [36]. The differential diagnosis is typically Parkinson's disease and Multiple System Atrophy due to the similar clinical presentation of these diseases in the early stages [2].

1.4 Pathological features of PSP

PSP is caused by damage and degeneration of neurons in certain parts of the brain including STN, substantia nigra, globus pallidus, putamen, pons, cerebellar white matter, dentate nucleus, caudate nucleus, and frontal and parietal lobes [2]. The hallmark pathology within these areas is the presence of intracellular deposits of hyperphosphorylated tau protein (p-Tau), particularly in the form of neurofibrillary tangles, however this disease is very heterogeneous both clinically and pathologically [2, 20]. The commonalities between most patients are the presence of p-Tau inclusions in the neurons of the cortex and within astrocytes, termed tufted astrocytes (TAs) [2, 20]. TAs are exclusive to PSP and are described as the accumulated tau protein branching from the cytoplasm to the proximal processes of

astrocytes in a thin, radial arrangement. For this thesis, the variants in tau pathology associated with PSP and other tauopathies will be referred to as pathological aggregates. Although some gene mutations are associated with the development of PSP in familial cases, these are rare and do not exist in sporadic patients [36].

1.4.1 Theories on the causes of PSP

One theory that is central to many neurodegenerative diseases is that once proteins start aggregating in one cell, it may cause connected cells to do the same, therefore spreading these toxic proteins throughout the central nervous system [36, 40]. This can be due to an unusual infectious agent that takes a certain period to produce visible effects. Moreover, it could be due to random gene mutations that occur in everyone all the time, occurring in a particular pattern in certain cells that then damage the cells resulting in protein dysfunction and aggregation [36, 40]. Understanding the composition of such protein aggregates can lead us to understanding the pathological mechanism that leads to their formation, including indications as to any genes that may need to be further investigated for their involvement.

1.5 Amyotrophic Lateral Sclerosis

Amyotrophic lateral sclerosis (ALS) is a progressive neurodegenerative disease of the upper and lower motor neurons (cerebral cortex and spinal cord respectively) [29, 58]. ALS is characterized by muscular weakness on onset, progressing to muscular dystrophy and eventual respiratory failure (usually 3-5 years after diagnosis) [57-58]. There is no effective treatment for ALS, with the only available drugs all acting to alleviate symptoms such as edaravone [19, 28] and Riluzole [10, 45], which adds only 3 months onto a patient's life expectancy. Sporadic ALS is 90% of cases, while familial ALS concerns the other 10% [48]. The pathological hallmark is understood to be protein aggregation in the cytoplasm of motor neurons, particularly of transactive response DNA-binding protein 43kDa (TDP-43) [48, 58]. Mutations in over 25 genes have been identified in association with fALS, such as *TARDBP* [56], *SQSTM1* [27], *VCP* [21], *OPTN* [32, 54, 55], *DCTN* [33, 41] and the most common mutations in *SOD1* [35] and *C9ORF72* [33, 48]. Notably, however, is that mutations in *TARDBP* occur in <5% of fALS cases, but the aggregated protein (TDP-43) is present in >97% of all ALS cases [31, 51], with the rest presenting with SOD1 pathology [5, 51].

Another gene with several mutations, termed *CCNF*, was first identified by Williams and colleagues in 2016 [58]. The S621G mutation of *CCNF* is found in both familial and sporadic ALS patients (Fig. 1), and this thesis will use fibroblasts from patients with this mutation. It should also be noted that proteostasis impairment has been associated with the aggregation of proteins in ALS [48], due to disruption in the protein quality control pathways such as unfolded protein response [18, 48], ubiquitin-proteasome system [27, 29, 48, 52] and the authophagy-lysosome pathway [49, 51].
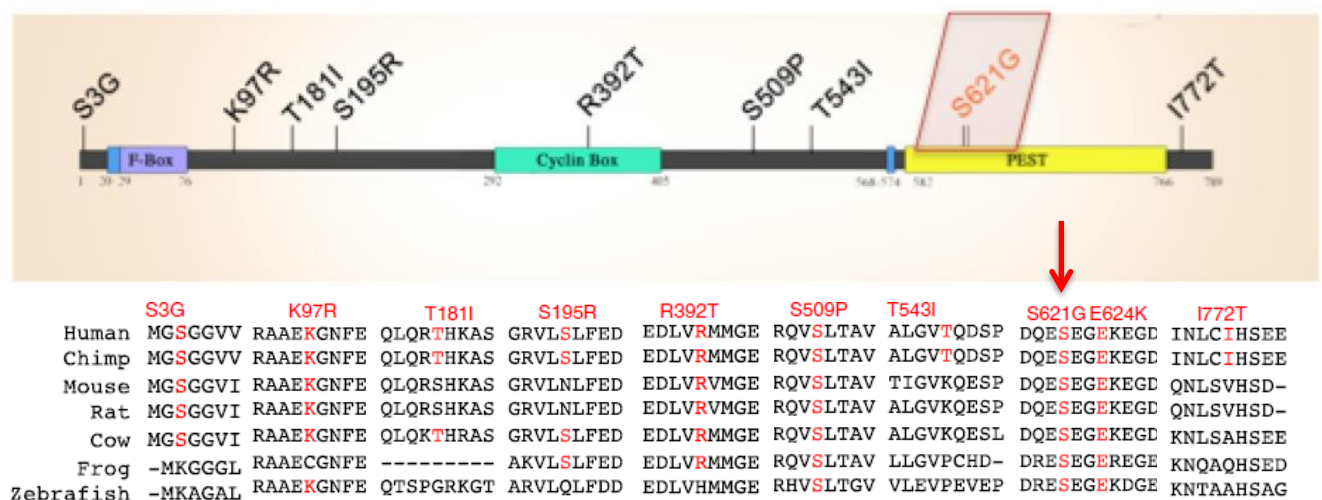
Fig. 1 Point mutations in *CCNF*, found by Williams and colleagues in 2016. These include S3G, K97R, T181I, S195R, R392T, S509P, T543I, S621G, and I772T. The focus of this project is on the S621G mutation, as marked. Figure taken from the article published by Williams et al. in 2016 [58]

1.6 Pathological protein aggregation provides insight into common molecular pathways that cause PSP and ALS

Although both diseases involve two functionally distinct and very different proteins (tau and TDP-43), there are common characteristic features that suggest that dysfunction in protein clearance pathways is involved in the formation of these aggregates [11, 18]. For example, the inclusions display a range of post-translational modifications [18, 52] such as hyperphosphorylation, ubiquitylation, and co-binding of proteins such as sequestosome-1 [39], SUMO [1, 24], heat-shock proteins [4], RNA binding proteins [15], etc. that play a role in protein clearance. Furthermore, impairment of the major intracellular protein degradation pathways (ubiquitin-proteasome system and autophagy) is not only implicated in PSP and ALS, but many other neurodegenerative diseases [16, 48].

1.7 The Study of the Molecular Composition of Protein Aggregates

There are a number of methods used to study the molecular composition of protein aggregates in both live cells and frozen or fixed tissue. These include biochemical extraction [37], protein purification [9], and proximity-ligation methods such as proximity-dependent biotinylation identification (BioID and BioID2) [22, 46-47] and ascorbate peroxidase (APEX and APEX2) [26, 43]. Biochemical extraction is associated with a significant sample loss, which is an important limitation to consider when working with tissue [3, 28]. The tissue is first homogenized, then cells are lysed using lysis buffer (that does not denature proteins) to release the proteins into solution. The proteins are then extracted using a range of separation-chemistry approaches (e.g. size or charge-based methods using chromatography columns with specific binding material to adsorb POIs), with recent developments using magnetic beads to easily facilitate repeated stages of protein capture. The tissue in this method is homogenized before the proteins are labeled, which is a limitation as this can disturb the structure and function of proteins and complex structures like inclusions, limiting accuracy and reliability [3, 6, 46]. Proximity-ligation methods are ideal in studying aggregates within live cells, whether that is to assess the history of protein-protein interactions (PPIs) (i.e. BioID) [45-46] or have a snapshot of PPIs (i.e. APEX) [26, 48]. However, these methods cannot be applied to fixed-tissue analysis and require the overexpression of a transgene to characterize the interactome of the POI instead of targeting the endogenous protein with antibodies. As conventional biochemical extraction and live cell methods are not ideal for obtaining accurate and reliable data from post-mortem patient tissue, a new method was recently devised by Bar and colleagues in 2018 [3] to overcome some of the limitations associated with the above methods. Additionally, this new method (termed biotinylation by antibody recognition) allows work on patient-derived cells without the addition of an artificial component (e.g. biotin ligase or soybean peroxidase tagged to the POI), which may affect the normal biological function of the POI.

1.8 Biotinylation by Antibody Recognition as a method for proximity-ligation detection of protein-protein interactions in fixed tissue

Biotinylation by antibody recognition (BAR) was devised for use on fixed post-mortem tissue and cells, and to identify "bait" proteins with the use of antibodies (instead of a fusion-tag) [3, 45-46]. The protein of interest (POI) is first labeled with a specific primary antibody,

before a secondary antibody is attached to facilitate biotinylation. When a horseradish peroxidase (HRP)-conjugated secondary antibody is in the presence of hydrogen peroxide (H_2O_2) and phenol biotin, it causes the biotinylation of proteins in direct vicinity to the POI (Fig. 2). When biotin is attached covalently to proximate proteins, harsh lysis buffer and high heat over an extended amount of time is necessary to reverse cross-link and solubilize proteins. Then, streptavidin-coated beads are used to remove biotinylated proteins, and Western blot (WB) and mass spectrometry (MS) are then used to detect and analyse these proteins.
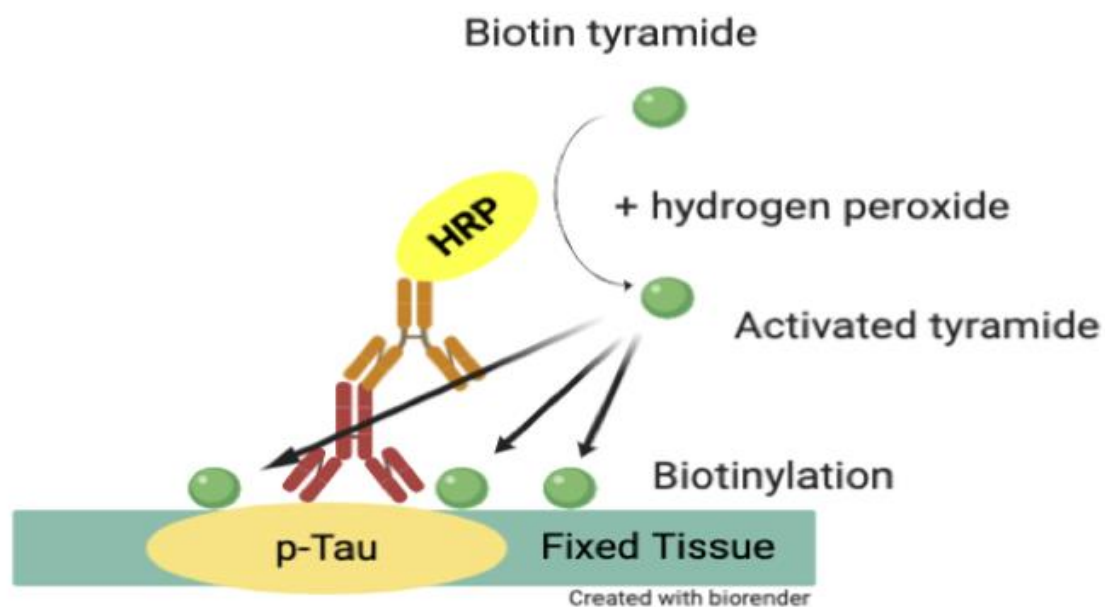
Fig. 2 How the BAR labeling occurs. Created with biorender.com

Additionally, BAR allows for the use of harsh lysis and extraction methods, providing more material to analyse and validate for more accurate and detailed findings. This will lead to better insight into the mechanisms at play within PSP and ALS based on the functions of the protein interactions identified. Since insoluble proteins and protein aggregates are the focus of this project, affinity purification (AP) [i.e. immunoprecipitation (IP)] is not a suitable alternative due to the method not allowing for harsh conditions to solubilize these proteins [3, 46-47]. IPs require the POI to be soluble in very specific buffers, which are usually weak detergent-based buffers containing little-to-no ionic detergents that break apart many PPIs. Most times the insoluble proteins can be solubilized but require harsh lysis buffers that contain ionic detergents (e.g. sodium dodecylsulfate) [49] and sometimes chaotrophic

reagents (such as urea) [24], which help to dissociate many interaction partners isolated by IP. However, the BAR method employs a biotin-streptavidin pull-down. This is one of the strongest bonds found in nature and streptavidin remains stable in various buffers including ionic detergents [14, 49]. Thus, this pull-down is useful for solubilizing insoluble proteins in harsher detergents. Streptavidin-conjugated bead pull-downs are used as a complement to proximity ligation methods to isolate the proteins after the strong binding between biotin and streptavidin has occurred. This technique will not only be carried out on fixed post-mortem brain tissue, but also fixed patient fibroblasts whilst maintaining a consistent method for all studies. A summary of the project workflow is outlined below (Fig. 3).

1.9 Project Aims

The **overall aim** of this project is to optimize the BAR method to identify the proteomic composition of pathological aggregates in postmortem PSP patient tissue and cultured fibroblasts from ALS patients.

1. Optimize the BAR technique for use in postmortem patient tissue and cultured patient fibroblasts.

2. Characterize the p-Tau aggregates labeled in patient brain tissue using mass spectrometry.

3. Characterize TDP-43 aggregates labeled in cultured patient fibroblasts using mass spectrometry.

1.10 Project Workflow
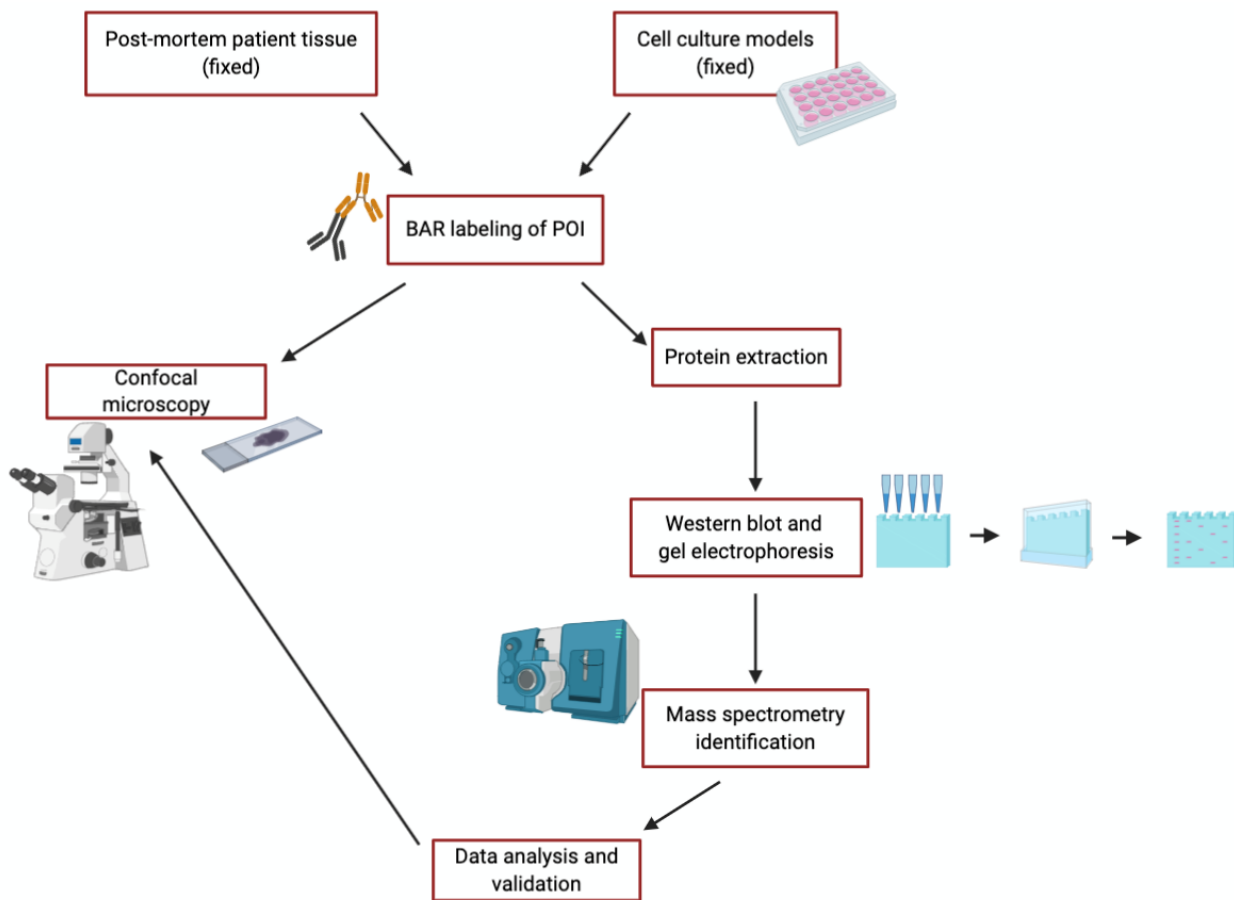
Fig. 3 Outline of the project workflow. Created with biorender.com

CHAPTER 2   Optimization of Biotinylation-by-Antibody Recognition (BAR) technique for fixed tissue and cells

2.1 Introduction

This chapter address aim 1 of this thesis in optimizing the BAR method for use in fixed tissue and cultured fibroblasts. The study of protein-protein interactions (PPIs) using the BAR method is new and, although it has been used before, a major part of the optimization process is to ensure the proteins-of-interest (POIs) could be labeled with biotin-SS-tyramide and selectively cleave off the tyramide-linked proteins. This step in the workflow is very important as the proteins are then selectively isolated using a reducing agent such as dithiothreitol (DTT), as is used here. This limits background noise that may come from streptavidin binding to non-specific proteins [8]. Moreover, the concentration of biotin is important, as it was found in our lab that higher concentrations lead to a larger labeling radius around the POI and can even label the entire cell, so various concentrations were tested. Further, DAPI staining protocol was optimized to properly label nuclei in tissue and cells for immunohistochemistry (IHC) imaging.

2.2 Methods

2.2.1 Cell culture

HEK293 cells were used for optimization purposes. HEK293 cells were grown in T75 flasks in Dulbecco's Modified Eagle Medium (DMEM) (Thermo Scientific) with 10% heat-inactivated foetal bovine serum (FBS) (Thermo Scientific), incubated at 37°C with 5% CO_2 and 95% humidity. Cells were grown to ~80% confluency before subculture. For subculture, the media was aspirated and the cells were washed with phosphate buffered saline (PBS) (Gibco™). Trypsin (Thermo Scientific) was used to detach cells from the flask before being split into two new T75 flasks or a 24-well plate (Corning®). For IHC, the cells were labeled with a primary antibody against importin-ß (Abcam) incubated for 20mins in DAPI of varying concentrations before being mounted onto glass slides with Prolong Antifade mountant. Additionally, varying concentrations of biotin-SS-tyramide were tested and imaged.

2.2.2 Tissue

Vibratome sections of rat brain tissue donated by Katherine Robinson from a methamphetamine study were used to optimize BAR on tissue. The sections were washed with TBS to remove agarose before endogenous peroxidases were quenched with 1% H_2O_2

for an hour at RT. Then, the sections were blocked with 10% normal goat serum (NGS) and 0.3M glycine in TBS for 2 hours at RT before being labeled with the primary antibody IbA1 (Abcam) diluted in 1% NGS (1:1000) at 4°C for 2 nights. Negative controls were incubated in 1% GS only, no primary antibody. Sections were washed and incubated with 4–5 drops of goat-conjugated superboost HRP overnight at 4°C. The next day, tissue sections were biotinylated at different concentrations diluted in 20X reaction buffer from the tyramide superboost kit (Invitrogen) for 45 mins at RT before adding 3µL of diluted H_2O_2 to each well to react for 95 seconds. Sodium ascorbate (500mM; Sigma-Alrich) stop solution was immediately added after biotinylation for 5 mins before the sections were washed and fluorescently tagged. Secondary antibodies conjugated with either Alexa 594 or Streptavidin 488 (Abcam) were diluted in 1% NGS (both 1:500) and left to incubated overnight at 4°C. Sections were stained with 3µM DAPI and mounted with ProLong^{TM} Glass Antifade mountant (Invitrogen).

2.2.3 Biotin Cleavage

Samples were placed into Eppendorf tubes and probe-sonicated 15 times at 40% power and 30% pulser using a Sonic Ruptor 250. Samples were reverse cross-linked by being heated at 95°C for 1 hour then at 60°C for another 2 hours. The samples were cooled to 4°C before the appropriate amount of 1X protease inhibitor cocktail (Roche) was added to each sample and centrifuged at 1000 rcf for 5 mins at 4°C. The supernatant was transferred to new tubes and 50µL of 2M urea was added to the initial sample tubes containing a pellet to examine how much protein did not make it into the clarified lysate. The samples were quantified using the bicinchoninic acid assay (BCA) kit (Thermo Scientific).

Equal amounts of protein were aliquoted and streptavidin-coated magnetic beads (Pierce™) were washed with radioimmunoprecipitation assay (RIPA) lysis buffer before 10µL was added to each sample. The samples were left on a rotating rack overnight at 4°C. Magnetic beads with the biotinylated proteins were isolated on a magnetic rack, and to reduce non-specific binding, these beads were wash with RIPA lysis buffer twice, once with 1M KCl, 1M Na_2CO_3, 2M urea, and finally twice with RIPA buffer.

2.3 Results

2.3.1 Overview of BAR Technique Optimization

At the commencement of this project, RR and SR had performed preliminary studies to establish the BAR technique. This included determination of which of the available patient tissue was of suitable quality for BAR labeling, as some cases were not suitable for this approach (e.g. over fixation or poor quality of postmortem tissue), and development of MS protocols for peptide analysis. For this project, it meant that all tissue used would be of sufficient quality and used pre-developed MS analysis protocols. This project was the first time that the research group had used BAR in fixed cultured cell samples, therefore the BAR-MS workflow was further developed in this project. The initial work by RR and SR used biotin-XX-tyramide, however the biotin-SS-tyramide (Iris Biotech) was trialed in this project to further optimize cleaving of biotinylated proteins that were captured by the streptavidin-conjugated beads.

2.3.2 Development of BAR labeling protocol for use with fixed cultured cells

This work extends from previously conducted work in the lab by RR and SR. Wild type (WT) HEK293 cells were used to optimize the BAR labeling technique for cell culture, which has not been performed previously in the lab. HEK293 cells were also utilized as material to learn the BAR labeling technique on before rat brain tissue was donated and used for practice of the technique in tissue. The primary antibody used for this step in cell culture was against importin-ß (Iß). Confocal images show appropriate staining of Iß, a nucleocytoplasmic shuttling protein located around the nucleus. Further, multiple biotin-SS-tyramide concenctrations were optimized in HEK293 cells. The concentration of biotin-SS-tyramide to be used was trialed at concentrations 10nM, 50nM, 100nM and 125nM. Images showed optimal biotinylation at 50nM based on specificity and signal of the biotin (Fig. 1). To ensure the same concentration of biotin-SS-tyramide can be applied in tissue sections as biotin-XX-tyramide, 50nM was tested on the rat brain tissue sections with the primary antibody against IbA1, which also showed appropriate staining of the microglia (Fig. 2). DAPI staining was optimised in HEK293 cells to 3µM in PBS, which is the same concentration used on the tissues. Iß and IbA1 markers were chosen in the early stages to validate the BAR labeling technique as these markers are ubiquitous and easy to visualize

under a microscope, allowing us to determine whether the biotin tagged the appropriate proteins within a close enough radius to the antibodies.
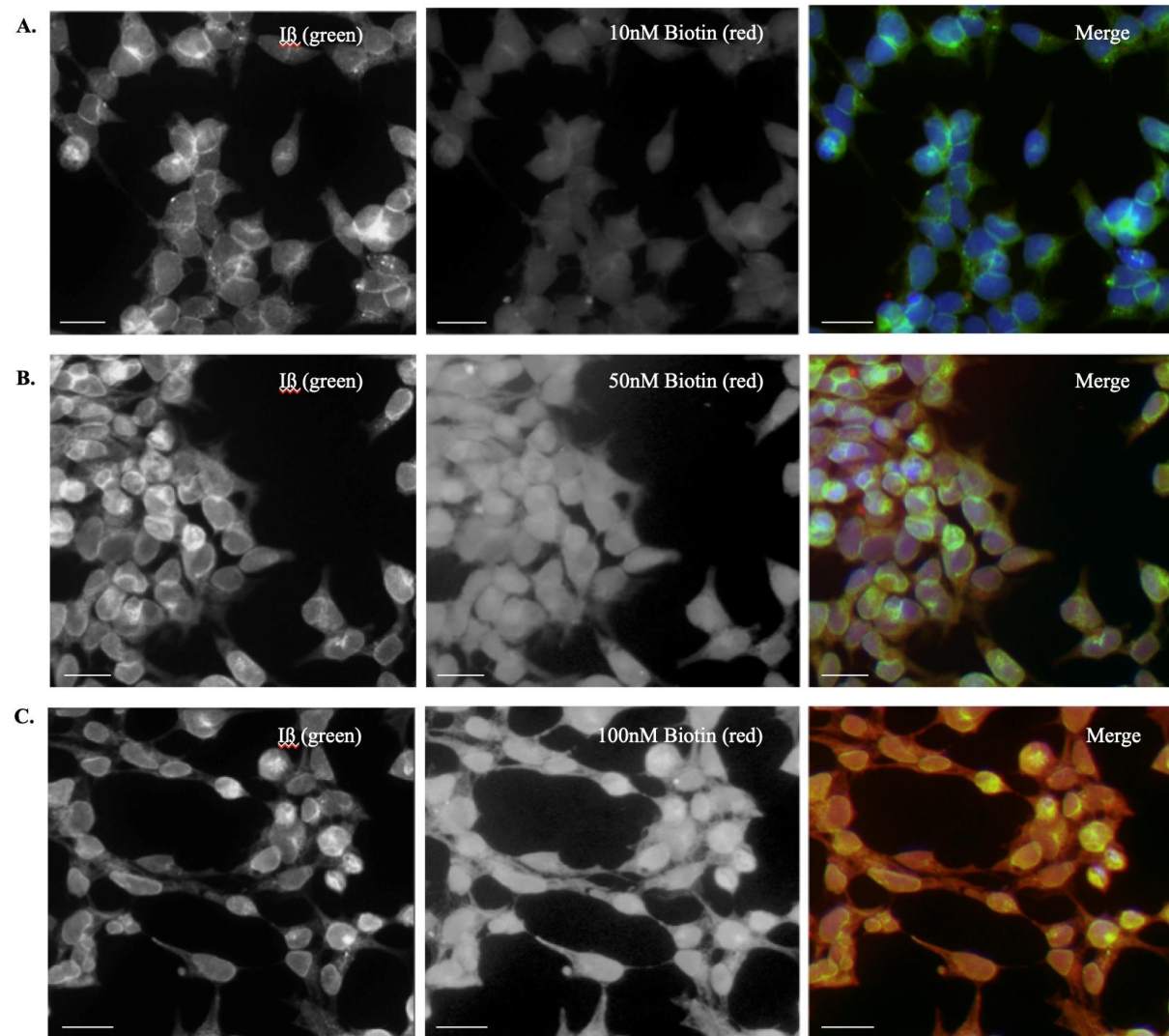
Fig. 1 Representative images of BAR labeling optimisation with varying concentrations of biotin-SS-tyramide in HEK293 cells. A. 10nM biotin shows a weak signal. B. 50nM biotin shows appropriate labeling of protein predominantly around nuclei with minimal non-specific binding.   C. 100nM biotin shows the cells are over-saturated with biotin, leading to lots of non-specific binding. This is especially within the cytoplasm as importin-ß is located (and shown labeled here) around the nucleus. Scale bars are 20μm
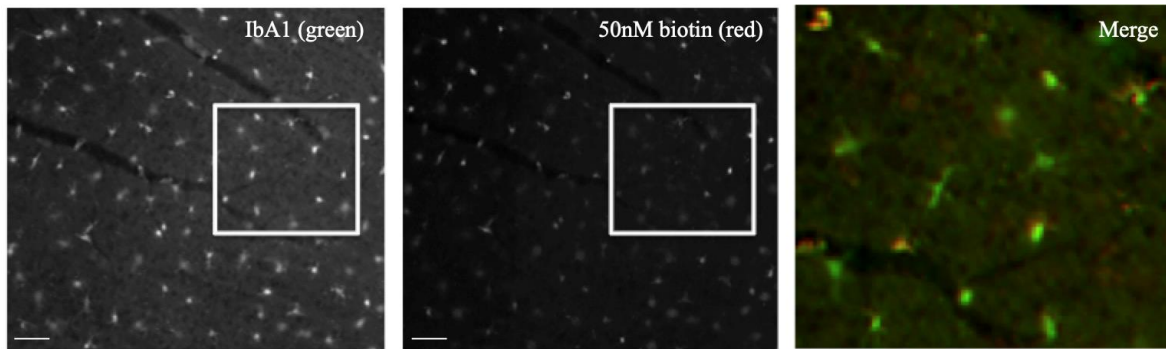
Fig. 2 Representative images of BAR labeling validation in fixed tissue with the use of 50nM of biotin-SS-tyramide for biotinylation in rat tissue sections. Shown here is co-localization of the primary antibody (IbA1) and biotin on microglia. Scale bars are 50μm

2.3.3 Biotin Cleavage

To determine the optimal concentration for biotin-SS-tyramide cleavage, 50mM and 100mM of DTT (Invitrogen) were tested [7]. The importance of cleaving biotinylated proteins from streptavidin beads is to ensure maximum sample is collected, as sample loss will yield incomplete data and skew the results. The samples with 100mM DTT appears to have cleaved more proteins in the positively labeled sample compared to the negative control than 50mM DTT, which cleaved around the same amount of protein in both samples (Fig. 3). Therefore, 100mM of DTT was used for all experiments conducted in the main project.
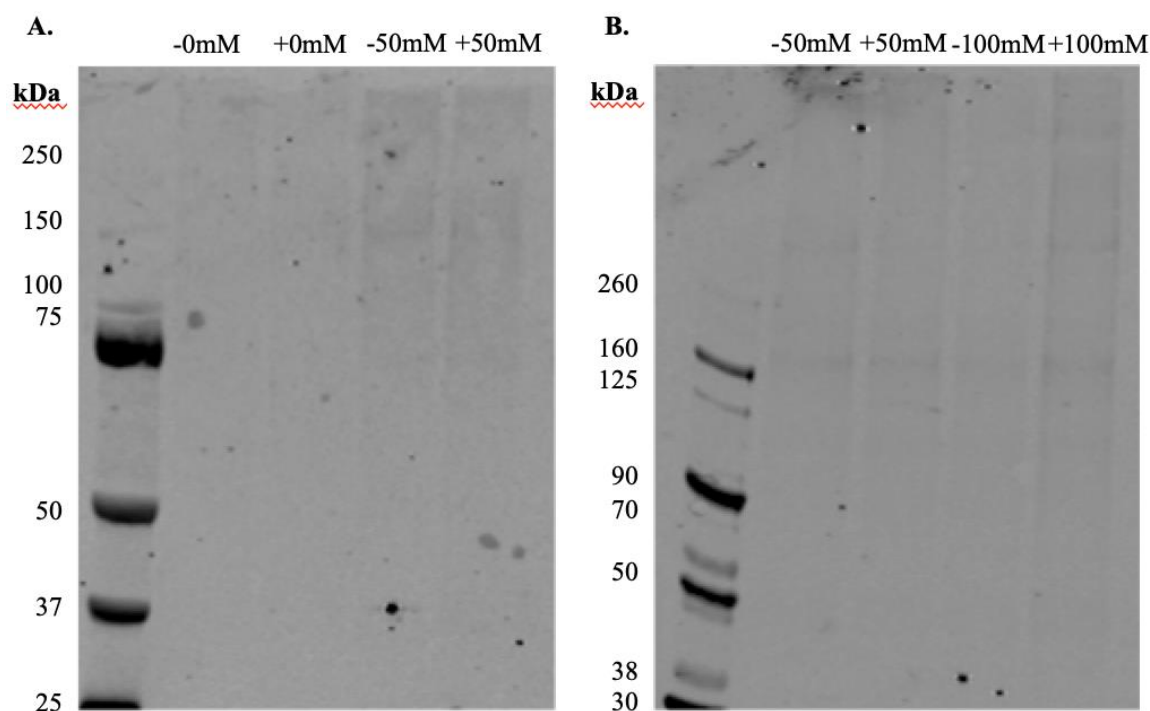
Fig. 3 Western blots show cleavage of biotinylated proteins at 50mM and 100mM. **A.** Cleaving of biotinylated proteins with 2 samples not incubated in DTT, and the other 2 samples incubated in 50mM DTT, and **B.** Cleaving of biotinylated proteins with 2 samples incubated in 50mM DTT, and the other 2 samples incubated in 100mM DTT

2.4 Discussion

In this chapter, we optimized BAR in rat brain tissue and HEK293 cells, which was used as a basis for later experiments in human brain tissue sections and patient-derived fibroblasts. Notably, the quality of the antibody [3, 23] used is important as a strong, appropriate bond and signal is crucial for this method to work and limits non-specific binding. To identify suitable antibodies, it is important for them to have been validated extensively in the literature, but will still need to be tested using the BAR technique. Fixed postmortem tissue requires significantly higher antibody concentration and incubation time than cultured cells (i.e. several days compared to overnight), as the antibody needs to penetrate through thicker tissue. As tissue preparation can vary greatly (e.g. thin microtome versus thick vibratome sections), incubation time needs to be optimized for different samples.

Cleaving biotinylated proteins from streptavidin beads properly is crucial to extract the biotinylated proteins for MS identification. If these proteins remain attached to the beads, it results in a significant sample loss and we may not get a fully representative proteomic

profile. Here, we showed that 50mM of DTT cleaves about the same amount of protein in both the negative control and positively labeled samples. This suggests that a 50mM concentration of DTT may not be effective in cleaving all the biotinylated proteins, but instead cleaves the non-specific bound structures that have been labeled with biotin. The 100mM DTT concentration appears to have a marked difference in the amount of protein that has been cleaved between the negative and positive samples, as well as more than what 50mM DTT appears to have cleaved. Therefore, 100mM DTT was the chosen concentration throughout the project. Although this concentration of DTT was chosen due to noticeable difference in protein yield, further optimizing to determine the plateau phase of protein capture will be necessary in the future. Higher concentrations of DTT may results in higher protein yield, which will be assessed in future experiments. Streptavidin-conjugated beads not only capture biotinylated proteins, but also random proteins may attach themselves to the beads. The disulfide bonds on the biotin-SS-tyramide provide a quick and easy way to specifically remove only biotinylated proteins [8, 30], therefore leaving unintentionally captured proteins behind. The overall BAR protocol for cells and tissue is different, and it is necessary to choose well-characterized antibodies for specific labeling. A further limitation of this method we found is that the protocols between different tissue types (i.e. muscle tissue, brain tissue, etc.) also vary, which means this is not a one-size-fits-all method and will have to be modified/optimized for each intended use.

CHAPTER 3   Biotinylation by Antibody Recognition to identify proteomic constituents of p-Tau inclusions in Postmortem Tissue: Progressive Supranuclear Palsy

Article I   Establishing a Proximity-Ligation Method to Understand the Interactome of phosphorylated-Tau aggregates in Progressive Supranuclear Palsy

This article has been prepared for journal submission at the time of thesis submission.

3.1 Chapter Introduction

Protein-protein interaction (PPI) studies in tissue samples typically rely on conventional biochemical extraction and co-immunoprecipitation methods [4, 17], which lend themselves to significant sample loss due to loss of structural integrity of cellular compartments and aggregate structures [11, 17, 20]. In this paper, BAR has been optimized to perform labeling in post-mortem PSP patient tissue to study the molecular composition of p-Tau aggregates, which addresses part of aim 1 in this thesis. The purpose of this aim is to establish an unbiased technique that selectively targets POIs with minimal sample loss to get a more in-depth understanding of the interactions of interest. Additionally, mass spectrometry workflow enabled us to analyse the proteins found in p-Tau aggregates as well as in close proximity, which may yield information on the formation of these aggregates. This addresses aim 2 of this thesis of characterizing p-Tau aggregate composition and formation.

The workflow of this part of the project is outlined in Fig. 2 within the paper. Optimization was conducted by RR, with the postmortem tissue labeled using the BAR technique conducted by RR (n = 12) and PS (n = 4). This was followed by validation through confocal imaging and immunoblotting, before the samples were processed through MS and generated protein lists analysed by PD 2.4 and IPA. The results arising from this study are presented in Article I.

3.2 Contributors

Method	Contributors	Specific Contributions
BAR optimization	RR, PS	RR optimized the BAR protocol used here. PS undertook additional optimization to develop the biotin cleavage and DAPI staining protocols.
BAR labeling	RR, PS	RR labelled 12 of the samples used for analysis, PS labelled 4 samples.

Confocal imaging	RR	All.
Immunoblotting	PS, SR	Primarily undertaken by PS under supervision and training of SR.
Mass spectrometry	PS, SR, FC	PS and SR prepared the samples for mass spectrometry analysis. FC ran the samples through the mass spectrometer and uploaded raw data to Proteome Discoverer 2.4.
Data analysis	PS, SR, AL, RC	Primarily undertaken by PS, with guidance from SR, AL and RC.
Manuscript write-up	PS, RC	Written by PS with the intellectual guidance of RC.

Establishing a Proximity-Ligation Method to Understand the Interactome of phosphorylated-Tau aggregates in Progressive Supranuclear Palsy

Paulina Szwaja[1], Rowan Radford[1], Stephanie Rayner[1], Albert Lee[1], Flora Cheng[1], Roger Chung[1]

[1]Department of Biomedical Sciences, Faculty of Medicine, Health and Human Sciences, Macquarie University

Correspondence:

paulina.szwaja@hdr.mq.edu.au

Abstract

Progressive supranuclear palsy (PSP) is a late-onset progressive neurodegenerative disease pathologically characterized by insoluble inclusions of phosphorylated-Tau (p-Tau) in neurons of the brain. Understanding the protein interactome of p-Tau inclusions may uncover important insight into PSP pathogenesis. Traditional biochemical extraction methods are typically biased with significant sample loss and non-specific binding. Thus to limit these problems, an unbiased proteomic approach was taken to label co-aggregating proteins within formalin-fixed post-mortem PSP. This approach, termed biotinylation by antibody recognition (BAR), is a recently described method that makes use of a primary antibody binding to the protein of interest (POI) and, with the addition of a secondary antibody conjugated to horseradish peroxidase, hydrogen peroxide and biotin tyramide, facilitates biotinylation of proteins proximal to the POI. Then the proteins are biochemically isolated and identified using mass spectrometry (MS). With this workflow and bioinformatic analysis, several proteins known to interact with p-Tau directly and indirectly have been identified along with potentially novel interactors. The data here substantiates the BAR-MS approach of rapidly labeling and identifying components of aggregates within fixed tissue with a broad application to other diseases and interaction studies.

Key words: Progressive supranuclear palsy; tau pathology, biotinylation, proximity ligation, mass spectrometry, neurodegeneration

Introduction

Progressive supranuclear palsy (PSP) is a progressive neurodegenerative disease clinically characterized by postural instability, mild dementia, slowing and stiffening of movement, and difficulty moving the eyes [19]. This disease affects around 5 out of 100,000 people, afflicting more men than women with signs typically presenting around age 60 [7, 15]. Disability from PSP occurs within 3–5 years of diagnosis and death within 6–12years, with pneumonia being the most common cause of death [15]. Currently, there is no treatment for PSP, however certain medications (e.g. levodopa) and other interventions are used to manage symptoms [15]. The pathological features of PSP include damage and degeneration of neurons above the nucleus within many parts of the brain including but not limited to pons, cerebellar white matter, substantia nigra, frontal and parietal lobes, and putamen [1]. Additionally, aggregation of hyperphosphorylated 4 repeat (4R) tau protein (p-Tau) is the hallmark pathology of the disease [1]. This classifies PSP as a tauopathy, particularly a primary tauopathy, which is defined as having tau as the main contributor to the pathology, compared to secondary tauopathies such as Alzheimer's disease (AD), where tau is associated with other pathologies, such as amyloid-ß in the case of AD [1].

PSP is quite heterogeneous both clinically and pathologically and may be difficult to distinguish, however most patients have the presence of p-Tau within astrocytes, termed tufted astrocytes (TAs), which are exclusive to PSP [1, 10]. Although some cases of PSP are associated with hereditary mutations in the gene microtubule associated protein tau (*MAPT*) that encodes for tau protein, these are quite rare [1, 15]. Additionally, more studies on the tau pathology are necessary to give a proper insight into how PSP is caused and progresses on a molecular level, which may provide some therapeutic targets.

The pathological hallmark of neurodegenerative diseases is the manifestation of insoluble protein aggregates [1, 8]. Composition and distribution of these aggregates define and identify such diseases like PSP, AD and Parkinson's disease. Aggregates were first characterized histopathologically in post-mortem tissue, complemented by biochemical extraction over the past 2 decades to develop a deeper understanding of the composition of these aggregates [17]. However, a big limitation of biochemical extraction is that the tissue must be homogenized before targeting the protein/s of interest. This may disturb the structure of proteins and aggregates, which limits accuracy and reliability. Additionally, this method is known to eventuate in significant samples loss. Bar et al. have developed a method in 2018

[3] that is stated to overcome some of the above stated limitations, termed biotinylation by antibody recognition (BAR). BAR was devised to be used on post-mortem patient tissue to identify proteins of interest (POIs) using a primary antibody (Fig. 1). After the primary antibody specific to the POI is added, a secondary antibody conjugated to horseradish peroxidase (HRP) is attached to facilitate biotinylation of proteins in close proximity to the POI after the addition of hydrogen peroxide and biotin tyramide. This allows investigation of protein aggregates not only in post-mortem tissue, but also experimental animal and cell culture models of the disease.
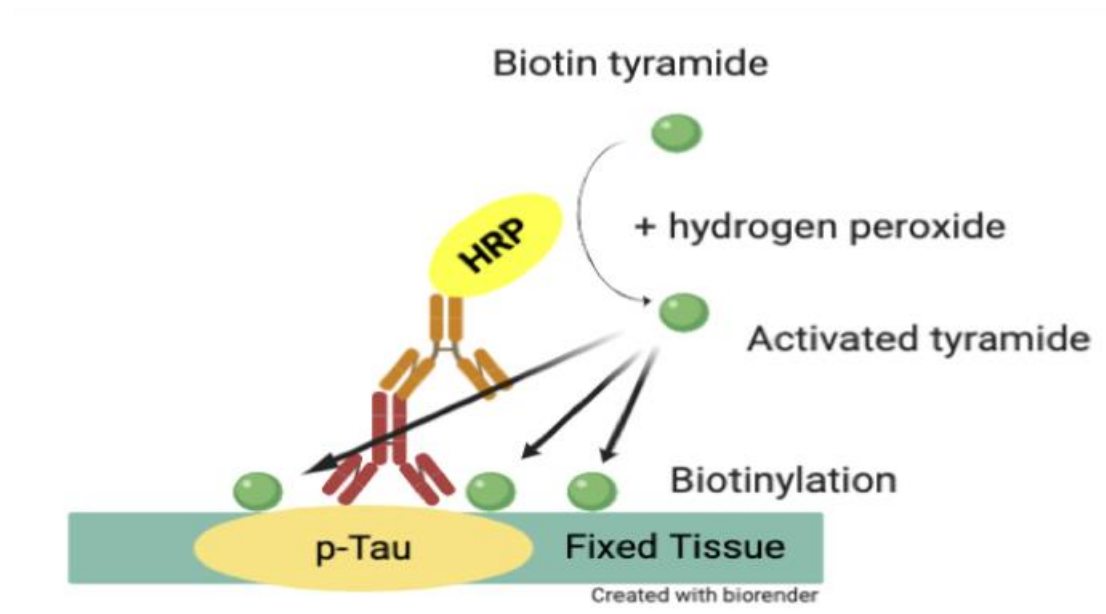
Fig. 1 The BAR labeling process at the molecular level

The BAR approach to protein-protein interaction studies, of labeling the POIs before tissue homogenization, significantly decreases the chance of non-specific binding and enhances likelihood of identification of the aggregate components. The overall aim of this study was to use BAR and MS to characterize the interactome of p-Tau aggregates in post-mortem tissue from PSP patients (Fig. 2).

34
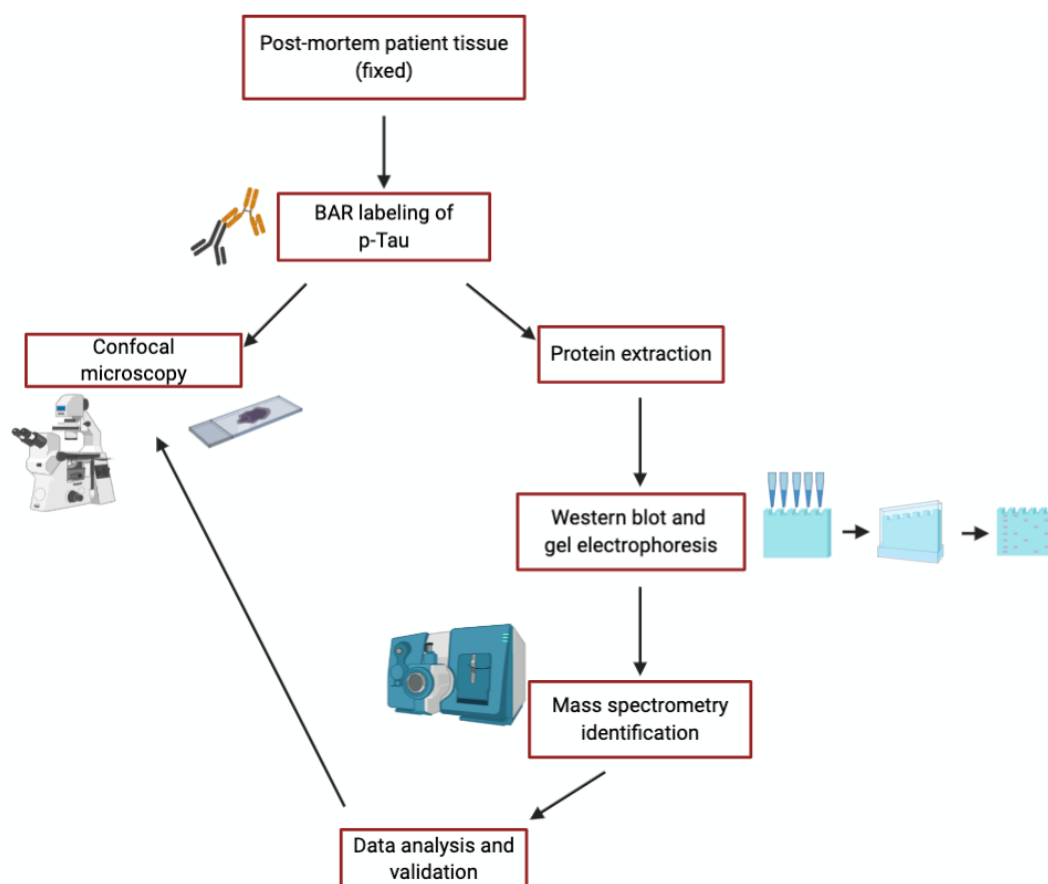
Fig. 2 Workflow of the project (first step needs to be reworked to not include cell culture)

Materials and Methods

The reagents used on the fixed postmortem PSP tissue is summarized in table 1.

Table 1. Summary of reagents used in this study

Reagents	Catalogue/Company	Concentration
Normal Goat Serum	G9023/Sigma-Aldrich	1% or 10% (v/v)
Anti-mouse Biotin-XX-tyramide SuperBoost™ Kit	B40911/ Invitrogen	N/A
Biotin-SS-tyramide	LS-3570.0250/Iris Biotech	50nM
DAPI	D1306/Life Technologies	3 µM
Prolong™ Glass	P36984/Life Technologies	N/A
Mouse anti-Phosphorylated Tau^{Thr221} (Monoclonal AT180)	MN1040/Invitrogen	1:500
Goat anti-mouse Alexa Fluor® 488	ab150117/Abcam	1:1000
Goat anti-mouse Alexa Fluor® 647	A21236/Invitrogen	1:1000

Post-mortem tissue

Post-mortem patient tissue of the motor cortex of 5 cases with PSP (table 2) was formalin-fixed and obtained from the South Australian Brain Bank under ethics approvals MSC/16/11/HREC and HREA 5201600387. The blocks were cut to 12mm^2 then sectioned using a Leica VTS1200 vibratome at 50-85 µm and stored in PBC-azine into 24-well plates. Each section was weighed prior to use.

Table 2: Patient cases of PSP used in this study

Case	Gender	Age (yrs)	PMI (hrs)	Duration (months)	Cause of Death	Clinical diagnosis	Neuropathology
0082	F	73	4	60	-	Corticobasal Degeneration	PSP
0095	M	73	4.5	60	-		PSP
0105	M	75	6	36	Aspiration pneumonia	Dementia with Lewy Bodies	PSP
0122	M	79	16	48	-		PSP
0136	F	80	17	72	-		PSP
	N=5 3:2 (M:F)	$76^{3.3}$ (avg.^{SD})	$9.5^{6.4}$ (avg.^{SD})	45.6			

BAR labeling

Endogenous peroxidases in postmortem patient tissue were quenched with 1.5% H_2O_2 in TBS for 1 hour at room temperature (RT). The sections were blocked with 10% goat serum for 2 hours at RT before applying the primary antibody diluted in 1% goat serum (1:1000 AT180) onto the sections and incubating them for 3 nights at 4°C. Sections were washed and the secondary antibody in 1% goat serum was added overnight at 4°C. The next day, tissue was incubated in 50nM biotinylation solution for 45min at RT before adding active biotinylation solution with 20X H_2O_2 for 1min. Sodium ascorbate (Sigma-Aldrich) stop solution (500mM) was immediately added and left for 1min before the tissue was washed with TBS, now ready for imaging and mass spectrometry preparation.

Confocal Imaging

Following BAR labeling, tissue sections were conjugated with secondary antibodies [Alexa Fluor 488 (1:1000) and Streptavidin-647 (1:1000)] before being stained with 3µM DAPI. The sections were then mounted onto glass slides using ProLong™ Glass Antifade mountant (Invitrogen) and imaged using Widefield fluorescence microscopy conducted on the Leica SP5x with resonant scanner confocal microscope.

Western Blot Analysis

Protein concentrations were determined with a Pierce™ BCA Protein assay kit. Equal protein amounts were aliquoted into the wells of 4-15% gradient SDS-PAGE gels (Invitrogen) in 1X loading buffer (Invitrogen) and separated by electrophoresis. Proteins were transferred onto a nitrocellulose membrane using the Trans-blot Turbo transfer system (Bio-Rad). Then, membranes were blocked for 30 minutes in 3% w/v bovine serum albumin (BSA) (Sigma-Aldrich) dissolved in PBS containing 0.05% v/v Tween at room temperature. The membrane was then incubated in streptavidin conjugated to a fluorophore (Invitrogen), diluted 1:1000 in 3% BSA blocking buffer. Images were taken using the Li-Cor Odyssey CLx Imaging System, and the images were analysed with ImageJ Studio Software.

Isolation of Aggregates/Pull-down

Tissue sections were homogenized using a hand-held douncer in BAR lysis buffer and probe-sonicated 15 times at 40% power and 30% pulser using a Sonic Ruptor 250. Samples were reverse cross-linked by being heated at 95°C for 1 hour then at 60°C for another 2 hours. The samples were cooled to 4°C before the appropriate amount of 1X protease inhibitor cocktail (Roche) was added to each sample and centrifuged at 1000 rcf for 5 mins at 4°C. The supernatant was transferred to new tubes and 50µL of 2M urea was added to the initial sample tubes containing a pellet to examine how much protein did not make it into the clarified lysate. The samples were quantified using the bicinchoninic acid assay (BCA) kit (Pierce™).

Equal amounts of protein were aliquoted and streptavidin-coated magnetic beads (Pierce™) were washed with radioimmunoprecipitation assay (RIPA) lysis buffer before 10µL was added to each sample. The samples were left on a rotating rack overnight at 4°C. Magnetic beads with the biotinylated proteins were isolated on a magnetic rack, and to reduce non-specific binding, these beads were washed twice with RIPA lysis buffer (1% NP-40, 0.1%

SDS, 50mM Tris HCl, 150mM NaCl, 0.5% Sodium Deoxycholate, 1mM EDTA and 0.01% sodium azide, pH of 7.4), once with 1M KCl, 1M Na_2CO_3, 2M urea buffer (2M urea, 10mM Tris-HCl), and finally twice with RIPA buffer.

Mass Spectrometry Preparation

In-gel trypsin digest

The biotinylated proteins were cleaved from the streptavidin beads using 100mM dithiothreitol (DTT) (Invitrogen). The samples were then loaded into 4%-12% Bis-Tris NuPAGE 10 well protein gels. The gels were run for 5 mins at 180V before the gels were taken out and left in Coomassie stain (Thermo Scientific) for 1-2 hours (until banding was seen). The gels were then de-stained in 25% methanol, with 2 solution changes over the first 2 hours, the left in fresh de-stain solution overnight. The gels were imaged using LiCor Odyssey CLx before the samples were cut from the gels into 1mm cubes and transferred into v-bottomed 96-well plates. The gels were further destained until Coomassie blue banding was barely visible, then incubated in 10mM DTT in 50mM AmBic (ammonium bicarbonate) at 37°C for 40 mins. Then the samples were alkylated with 20mM IAA in 50mM AmBic for 40 mins at room temperature in the dark. Once the samples were dry, 10µg/mL of sequencing grade trypsin in 50mM AmBic was added to each and incubated overnight at 37°C. The resulting peptides were transferred to new tubes and lyophilized in a Speedvac.

Sample purification

C18 OMIX tips (Agilent) were pre-washed and equilibrated to desalt peptides once suspended in 0.1% formic acid (FA). The peptides were lyophilized again in a Speedvac before being prepared for MS analysis.

Mass Spectrometry

The lyophilized peptides were again resuspended in 0.1% FA and centrifuged at 14,000 rcf for 15 minutes to remove insoluble debris. The clarified peptides were added to glass vials and analysed by LC-MS/MS. Peptides were separated with the Ultimate 2000 nanoLC (Thermo Scientific) fitted with an Acclaim PepMap RSLC column (Thermo Scientific) on a 120 minute gradient with a flow rate of 300nL/min (2-95% v/v AcN, 0.1% v/v FA). Eluted peptides from nano LC column were ionized into the Q Exactive Plus mass spectrometer (Thermo Scientific). A 10µm emitter tip was fitted to the electrospray source with the electrospray voltage maintained at 1.5kV (New Objective, Woburn, MA). The capillary

temperature was set to 25°C. The precursor ions for MS/MS fragmentation were selected using a data-dependent "top 15" method running in FT-FT acquisition mode with HCD fragmentation. The FT-MS analysis was performed at 70,000 resolution and a 1×10^6 ions AGC target in full MS. MS/MS scans were performed at 35,500 resolution and a 2×10^5 ions AGC target. Injection times were set to a maximum of 121 milliseconds. For triggering MS/MS fragmentation, the ion selection threshold was set to 25,000 counts, and a 1.4 m/z isolation width and normalized collision energy of 27 were employed to perform HCD fragmentation.

Bioinformatics and Statistics

The MS data obtained from the tissue samples were first analysed in Proteome Discoverer (PD) 2.4 (Thermo Scientific). The peptides were searched against the *Homo sapiens* SwissProt database with the following parameters. Trypsin as the enzyme, with a maximum of three missed cleavage sites allowed. The precursor mass tolerance was set to 20ppm and fragment mass tolerance set to 0.1 Da. The maximum equal modification was set at three per peptide, with dynamic modifications set to oxidation of methionine, biotinylation of lysine and N-terminus of protein, and acetylation of N-terminus. The static modification used was carbamidomethylation modification of cysteine, and normalization was set to none. Data was further process in a Label-Free Quantitation (LFQ) workflow using the Minora Feature node and percolator node. The latter node estimates false discovery rates at the protein level through an incorporated decoy database. Additionally, the percolator node was used for FDR estimations at the peptide-to-spectrum matches (PSMs) level. Results were adjusted for final global FDR to be less than 1% at both peptide and protein levels, and proteins were listed if 2 or more unique peptides were identified. A requirement for validation of protein identifications was a q-value <0.01.

The data generated here was exported into Microsoft Excel, where the data was further filtered using abundance ratios that had a fold change of >1.5 and <0.5. This data was then input to Ingenuity pathway analysis (IPA) (QIAGEN) to characterize and classify the identified proteins and their interaction partners according to molecular function. For this, a right-tailed Fischer's Exact Test was used. Statistically significant results were considered to be at a p-value ≤0.05.

Results

Selective biotinylation of proteins proximal to p-Tau aggregates in PSP tissue

To biotinylate proteins within p-Tau inclusions in post-mortem PSP tissue, we first targeted p-Tau with a monoclonal antibody that targets the tau phosphorylation site at threonine 231 (antibody AT180). Then secondary antibody conjugated to poly-HRP was added to bind to the primary antibody and facilitate biotinylation with the addition of H_2O_2 and biotin-SS-tyramide to the samples. Negative controls did not contain the primary antibody. Confocal images show the presence of successful biotinylation in tau-targeted samples compared to negative controls (Fig. 3 and Fig. 4). Furthermore, there was a clear overlap of biotin and p-Tau, indicating successful antibody-targeted biotinylation of the aggregate and vicinal proteins. Visual comparison indicates that AT180 labels mature tangles whereas AT8 labels more stages of pathology (not published).

Characterization of p-Tau aggregates using BAR in PSP tissue

Following BAR labeling, the post-mortem tissue was homogenized and the biotinylated proteins were isolated using a streptavidin column. These proteins were run through a NU-PAGE gel and were excised to gel purify the proteins in preparation for MS analysis. We noted the presence of numerous protein bands in the BAR-labeled samples, many of which were absent or quite faint in the negative control samples where the AT180 antibody was omitted (Fig. S1).

MS analysis generated a list of proteins identified in each sample. IPA was used to perform bioinformatic analysis of these lists to characterize the interactome of p-Tau inclusions. Initially, the raw protein lists were filtered to show proteins with an abundance ratio (AR) at the standard cut-off (AR >1.5 fold relative to control). The total number of proteins found in this list is 500. Due to such a high number of proteins, the lists were further filtered based on their relevance to PSP and tauopathies using Bioprofiler in IPA (table 4), which characterizes proteins based on their disease functions using current literature. These final lists were compared to the raw data to see how well the BAR method worked in identifying all the appropriate proteins in the raw data. The proteins in each sample are listed, with extra columns to identify common proteins amongst 3, 4 and 5 samples, to indicate significance of the findings. Only 2 proteins-of-interest (POIs) with AR>1.5 were found in all 5 samples,

with 14 proteins in 4 samples and 39 in at least 3 samples. Additionally, BAR may have also identified novel interactors of p-Tau that will need further validation (table S1).
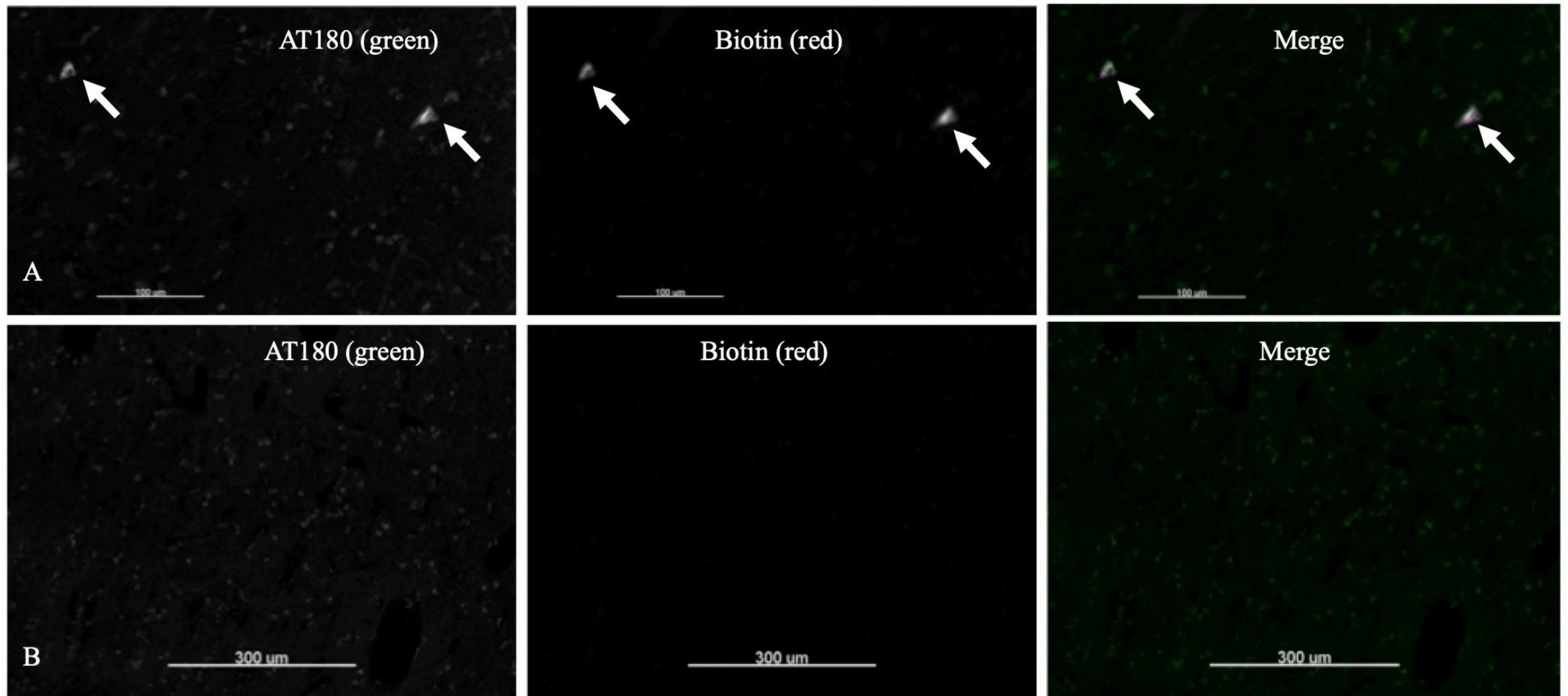
Fig. 3 Confocal images (10X magnification) of BAR-labeled postmortem PSP tissue (patient ID: 122). **A.** Biotin labeling of tissue following pre-labeling with primary antibody against p-Tau (AT180). Two examples of p-Tau pathology with strong intense labeling are shown (arrows). The images also show low level of tissue auto-fluorescence. **B.** Biotin labeling of negative control without AT180 antibody. These images show dull background auto-fluorescence only
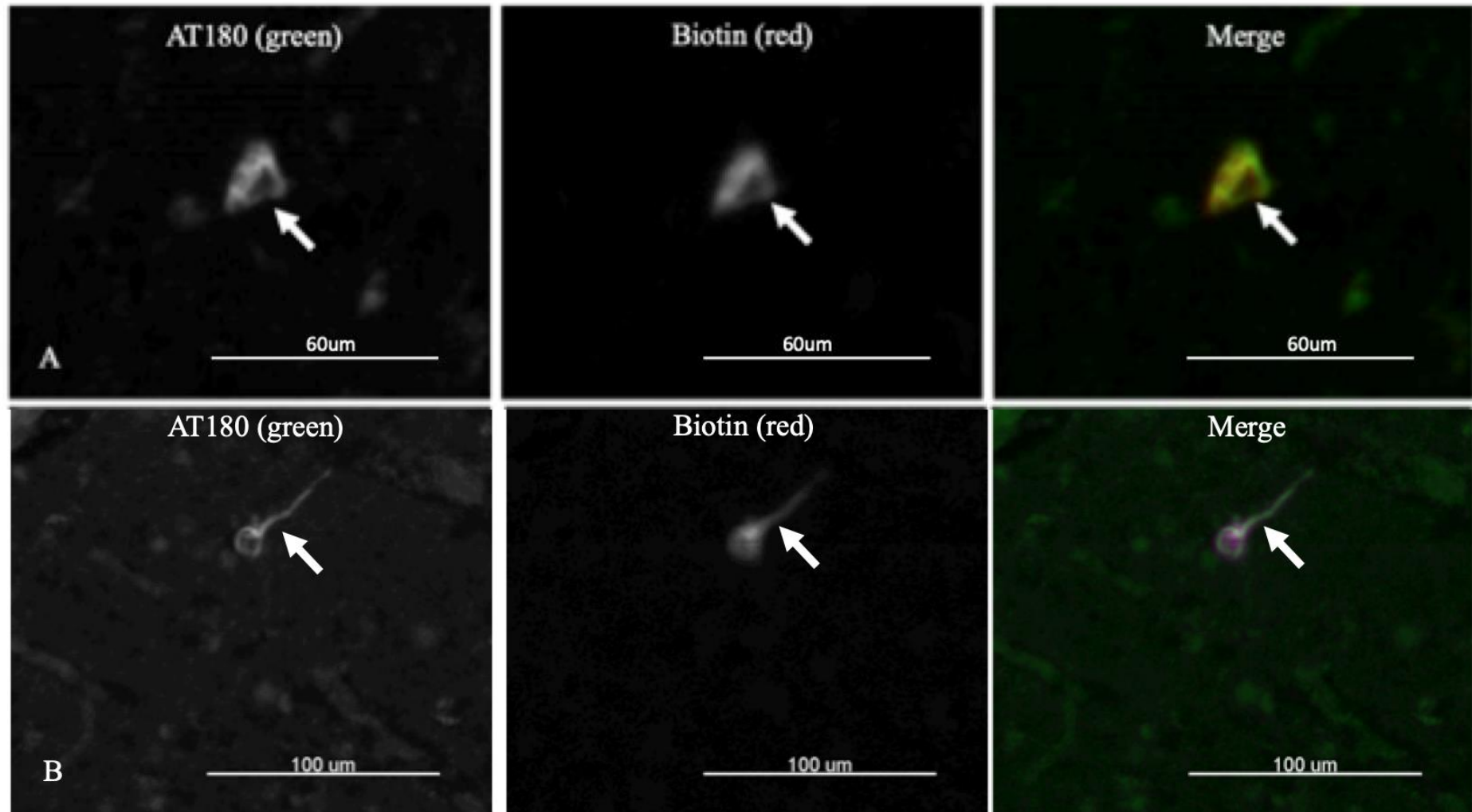
Fig. 4 Two examples of p-Tau pathology in postmortem PSP tissue labeled with AT180. Zoomed in images of the image in Fig. 3A show co-labeling of the AT180 antibody and biotin, which indicates the BAR-labeling works appropriately. **A.** Shows a neurofibrillary tangle stuck inside the cytoplasm. **B.** Shows a dystrophic neurite

Table 4 Proteins identified using IPA found in a set number of samples at an AR of at least 1.5

Found in 3 samples				Found in 4 samples		Found in 5 samples
Clusterin	Tubulin beta-3 chain	Rab GDP dissociation inhibitor alpha (GDI1)	Spectrin alpha chain, non-erythrocytic 1	Alpha-synuclein	Dihydropyrimidinase-related protein 2	L1 cell adhesion molecule
Vesicle-associated membrane protein 2	Microtubule-associated protein 2	Tubulin alpha-1A chain	Dihydropyrimidinase-related protein 2	Prion protein	Receptor of activated protein C kinase 1	Valosin-containing protein
Voltage-dependent anion-selective channel protein 1	Immunoglobulin heavy constant gamma 1 IGHG1	Alpha-synuclein	Receptor of activated protein C kinase 1	Growth-associated protein 43	L1 cell adhesion molecule	
Apolipoprotein D	Guanine nucleotide-binding protein G(I)/G(S)/GO) subunit gamma-3	Prion protein	L1 cell adhesion molecule	Apolopoprotein 3	Valosin-containing protein	
Heterogeneous nuclear ribonucleoproteins A2/B1	Tubulin alpha-4A chain	Growth-associated protein 43	Valosin-containing protein	DJ-1		
Superoxide dismutase 2 [mitochondrial]	Serine/threonine-protein phosphatase 2B catalytic subunit alpha isoform	ATP citrate lyase	**Amphiphysin**	ATP citrate synthase		
Complement C3	Beta-soluble NSF attachment protein NAPB	DJ-1	Band 4.1-like protein 3	Neurogranin		
NAD(P) transhydrogenase, mitochondrial	Contactin associated protein 1	ATP citrate synthase	Microtubule-associated protein 1B	Neuronal cell adhesion molecule		

Transcriptional activator protein Pur-alpha	1-phosphatidylinositol 4,5-bisphosphodiesterase beta-1	Neurogranin	Microtubule-associated protein 1B	
Contactin 1	Calcium/calmodulin-dependent protein kinase type II subunit-α	Neuronal cell adhesion molecule	Spectrin alpha chain, non-erythrocytic 1	

Notably, several patients displayed p-Tau inclusions with relatively few other abundant proteins, while other patients displayed p-Tau inclusions with complex proteomic profiles of over 20 proteins. Furthermore, some of the proteins identified by Bioprofiler (IPA) are not directly related to PSP or tauopathies (e.g. GDI1 is related to seizures only [24]), while the others are related in terms of ataxia and other gait problems, which are common in PSP and related diseases.

Discussion

This study demonstrates BAR as an unbiased proteomic approach to determine pathological tau aggregate composition in a non-disruptive manner. Insights into the proteomic profile of tau aggregates identify potential physiological mechanisms that play a pathological role in disease formation of PSP. In this article, we elucidate proteins associated with tau within the aggregate and in close proximity to known and potentially novel interactors. Notably, proteins such as alpha-synuclein [26], DJ-1 [2, 12, 16], clusterin [6, 28], and valosin-containing protein [14, 27] appeared in the filtered lists, which are commonly reported proteins involved in various tauopathies. The increase in many of these proteins in 3 or more samples suggests their implication in the disease process of PSP as well. Mapping the proteomic profile of p-Tau inclusions in PSP postmortem patient tissue may provide insight into this problem by identifying what mechanisms are at play, how they may interact and to work backwards to understand how p-Tau inclusions were formed.

A standard threshold of AR>1.5 presented 38 proteins in 3 or more samples, giving confidence of their involvement with tau. However, just because some proteins are found to be of lower abundance does not necessarily mean that they are not significant, they may just naturally be less abundant and less involved in the disease process, but involved nonetheless. This will need to be investigated further by standard immunohistochemistry (IHC) along with co-immunoprecipitation assays to validate their interaction with tau, whether direct or indirect. Importantly, p-Tau was found in the raw data of 4-out-of-5 samples, however it did not meet the AR threshold even though it was expected to be the most abundant protein, and there may be several reasons for this. The primary antibody used (AT180) [22] appears to label only mature pathology compared to the AT8 antibody [23] used by RR and SR that appears to label all stages of pathology. Additionally, p-Tau may not have been properly

cleaved from the streptavidin beads, which requires further optimization. Furthermore, tau inclusions are a mixture of soluble and insoluble proteins, therefore future modification to the BAR protocol is needed to include differential processing to allow analysis of both fractions, not just the proteins soluble in the BAR lysis buffer analysed here.

Analysis of the proteomic data was simplified by the use of IPA in filtering the data for proteins associated with tauopathies (including PSP) and neurodegeneration, however this does come with some limitations. Important proteins known to be involved in tauopathies and other neurodegenerative processes did not appear in the final filtered lists, such as heat-shock proteins (Table S1). When accepting to include proteins associated with disease and phenotype, a few of these show up (not all), however proteins completely unrelated to tauopathies and neurodegeneration appear (such as GDI1, which is involved in seizures [24]). Conversely, this data illustrates that most patients do not have pure p-Tau pathology, but a mixture (e.g. p-Tau and amyloid-ß) as many patients have comorbid diseases such as Alzheimer's disease and frontotemporal dementia. This is further validated by table S2, which shows proteins related to other disease pathologies not necessarily related to tauopathies. BAR should be used with caution and as a quick scan through of what the data holds then refer back to the full list for anything that may have been missed. This still allows for easier analysis of data as IPA presents most of the important proteins with relevant articles they are associated with.

Some studies that have biochemically-extracted inclusions from postmortem tissue of patients with tauopathies (i.e. Alzheimer's Disease and Parkinson's Disease) found that these inclusions contain proteins that have a neurotoxic affect on neuronal cells leading to neurodegeneration and dysfunction [5, 21, 26]. However, these properties were not always replicated in synthetic inclusions of the same kind [9, 25]. This indicates that specific features and mechanisms of disease may only be studied in patient-derived tissue. Overall, this paper illustrates the efficacy of the BAR-MS workflow in characterizing pathological tau aggregates quickly and in a non-disruptive manner. Further validation of the data will provide significant insight into the mechanisms at play within PSP, answering some pertinent questions within the field. The BAR method can also be broadly applied in research for various interaction studies in tissue after thorough optimization.

References

1. Arendt T, Stieler JT, Holzer M (2016) Tau and tauopathies. Brain Research Bulletin 126:238-292. doi:10.1016/j.brainresbull.2016.08.018

2. Ariga H (2017) DJ-1/PARK7 Protein: Parkinson's Disease, Cancer and Oxidative Stress-Induced Diseases, vol 1037. Singapore: Springer Singapore, Singapore. doi:10.1007/978-981-10-6583-5

3. Bar DZ, Atkatsh K, Tavarez U, Erdos MR, Gruenbaum Y, Collins FS (2017) Biotinylation by antibody recognition: a method for proximity labeling. Nature methods 15. doi:10.1038/nmeth.4533

4. Cuatrecasas P, Wilchek M, Anfinsen CB (1968) Selective Enzyme Purification by Affinity Chromatography. Proceedings of the National Academy of Sciences of the United States of America 61:636-643. doi:10.1073/pnas.61.2.636

5. Dugger BN, Dickson DW (2017) Pathology of Neurodegenerative Diseases. Cold Spring Harbor perspectives in biology 9. doi:10.1101/cshperspect.a028035

6. Foster EM, Dangla-Valls A, Lovestone S, Ribe EM, Buckley NJ (2019) Clusterin in Alzheimer's Disease: Mechanisms, Genetics, and Lessons From Other Pathologies. Frontiers in Neuroscience 13. doi:10.3389/fnins.2019.00164

7. Golbe LI (2014) Progressive supranuclear palsy. Seminars in neurology 34:151-159. doi:10.1055/s-0034-1381736

8. Heemels M-T. (2016) Neurodegenerative diseases. Nature 539:179. doi:10.1038/539179a

9. Ingelsson M (2016) Alpha-Synuclein Oligomers-Neurotoxic Molecules in Parkinson's Disease and Other Lewy Body Disorders. vol 10. doi:10.3389/fnins.2016.00408

10. Jadhav S, Avila J, Scholl M, Kovacs GG, Kovari E, Skrabana R, Evans LD, Kontsekova E, Malawska B, de Silva R, Buee L, Zilka N (2019) A walk through tau therapeutic strategies. Acta Neuropathologica Communications 7. doi:10.1186/s40478-019-0664-z

11. Kim DI, Jensen SC, Noble KA, Kc B, Roux KH, Motamedchaboki K, Roux KJ

(2016) An improved smaller biotin ligase for BioID proximity labeling. Molecular biology of the cell 27:1188-1196. doi:10.1091/mbc.E15-12-0844

12. Kumaran R, Kingsbury A, Coulter I, Lashley T, Williams D, de Silva R, Mann D, Revesz T, Lees A, Bandopadhyay R (2007) DJ-1 (PARK7) is associated with 3R and 4R tau neuronal and glial inclusions in neurodegenerative disorders. Neurobiology of Disease 28:122-132. doi:10.1016/j.nbd.2007.07.012

13. Lam SS, Martell JM, Kramer KJ, Deerinck TJ, Ellisman MH, Mootha VK, Ting AY (2014) Directed evolution of APEX2 for electron microscopy and proximity labeling. Nature methods. doi:10.1038/nmeth.3179

14. Mori F, Tanji K, Toyoshima Y, Sasaki H, Yoshida M, Kakita A, Takahashi H, Wakabayashi K (2013) Valosin-containing protein immunoreactivity in tauopathies, synucleinopathies, polyglutamine diseases and intranuclear inclusion body disease. Neuropathology 33:637

15. National Institute of Neurological Disorders and Stroke (2020) Progressive Supranuclear Palsy Fact Sheet. NINDS. https://www.ninds.nih.gov/Disorders/Patient-Caregiver-Education/Fact-Sheets/Progressive-Supranuclear-Palsy-Fact-Sheet

16. Neumann M, Müller V, Görner K, Kretzschmar H, Haass C, Kahle P (2004) Pathological properties of the Parkinson's disease-associated protein DJ-1 in α-synucleinopathies and tauopathies: relevance for multiple system atrophy and Pick's disease. Acta Neuropathologica 107:489-496. doi:10.1007/s00401-004-0834-2

17. Ngounou Wetie AG, Sokolowska I, Woods AG, Roy U, Loo JA, Darie CC (2013) Investigation of stable and transient protein-protein interactions: Past, present, and future. vol 13. doi:10.1002/pmic.201200328 [SEP]

18. Rhee H-W, Zou P, Udeshi ND, Martell JD, Mootha VK, Carr SA, Ting AY (2013) Proteomic mapping of mitochondria in living cells via spatially restricted enzymatic tagging. Science (New York, NY) 339:1328-1331. doi:10.1126/science.1230593

19. Richardson JC, Steele J, Olszewski J (1963) Supranuclear ophthalmoplegia, pseudobulbar palsy, nuchal dystonia and dementia. A clinical report on eight cases of "heterogenous system degeneration". Transactions of the American Neurological Association 88:25-29

20. Roux KJ, Kim DI, Burke B (2013) BioID: A Screen for Protein-Protein Interactions. Current Protocols in Protein Science 74:19.23.11-19.23.14. doi:10.1002/0471140864.ps1923s74

21. Shankar GM, Li S, Mehta TH, Garcia-Munoz A, Shperadson NE, Smith I, Brett FM,

Farrell MA, Rowan MJ, Lemere CA, Regan CM, Walsh DM, Sabatini BL, Selkoe DJ (2008) Amyloid-ß protein dimers isolated directly from Alzheimer's brains impair synaptic plasticity and memory. Nature Medicine 14:837. doi:10.1038/nm1782

22. Strang K, Goodwin M, Riffe C, Moore B, Chakrabarty P, Levites Y, Golde T, Giasson B (2017) Generation and characterization of new monoclonal antibodies targeting the PHF1 and AT8 epitopes on human tau. Acta Neuropathologica Communications 5. doi:10.1186/s40478-017-0458-0

23. Taniguchi-Watanabe S, Arai T, Kametani F, Nonaka T, Masuda-Suzukake M, Tarutani A, Murayama S, Saito Y, Arima K, Yoshida M, Akiyama H, Robinson A, Mann D, Iwatsubo T, Hasegawa M (2016) Biochemical classification of tauopathies by immunoblot, protein sequence and mass spectrometric analyses of sarkosyl-insoluble and trypsin-resistant tau. Pathology and Mechanisms of Neurological Disease 131:267-280. doi:10.1007/s00401-015-1503-3

24. Wang J, Lin Z-J, Liu L, Xu H-Q, Shi Y-W, Yi Y-H, He N, Liao W-P (2017) Epilepsy-associated genes. Seizure: European Journal of Epilepsy 44:11-20. doi:10.1016/j.seizure.2016.11.030

25. Wang Z, Jackson RJ, Hong W, Taylor WM, Corbett GT, Moreno A, Liu W, Li S, Frosch MP, Slutsky I, Young-Pearse TL, Spires-Jones TL, Walsh DM (2017) Human Brain-Derived Aß Oligomers Bind to Synapses and Disrupt Synaptic Activity in a Manner That Requires APP. The Journal of neuroscience : the official journal of the Society for Neuroscience 37:11947-11966. doi:10.1523/JNEUROSCI.2009-17.2017

26. Wong CY, Krainc D (2017) α-synuclein toxicity in neurodegeneration: mechanism and therapeutic strategies. Nature Medicine 23:1. doi:10.1038/nm.4269

27. Yabe I, Yaguchi H, Kato Y, Miki Y, Takahashi H, Tanikawa S, Shirai S, Takahashi I, Fujioka S, Watanabe M, Nakagawa S, Kunieda Y, Ikeda Y, Hasegawa M, Nishihara H, Tanaka S, Tsuboi Y, Hatakeyama S, Wakabayashi K, Sasaki H (2017) Mutations in bassoon in individuals with familial and sporadic progressive supranuclear palsy-like syndrome. Journal of the neurological sciences 381:1048-1049. doi:10.1016/j.jns.2017.08.2962

28. Zhou Y, Hayashi I, Wong J, Tugusheva K, Renger JJ, Zerbinatti C (2014) Intracellular Clusterin Interacts with Brain Isoforms of the Bridging Integrator 1 and with the Microtubule-Associated Protein Tau in Alzheimer's Disease.(Research Article). PloS one 9. doi:10.1371/journal.pone.0103187
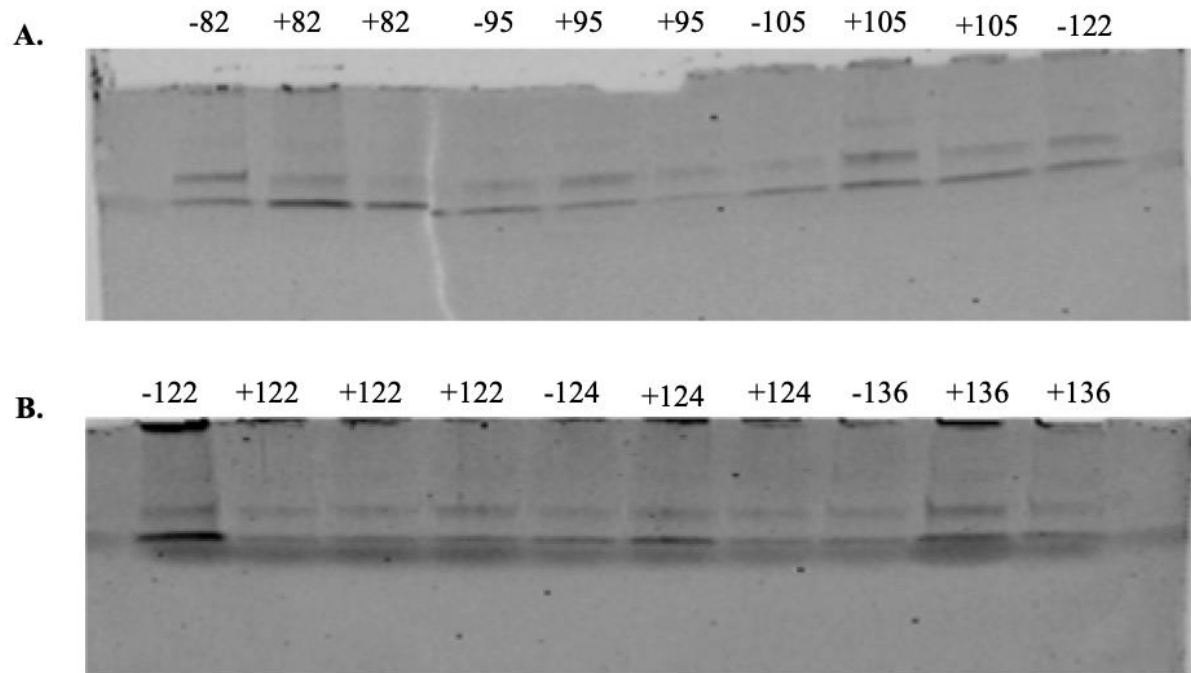
Fig. S1 MS gels containing isolated protein samples from PSP samples with (+) and without (-) primary antibody AT180. Images taken with LiCor Odyssey CLx. Patient ID 124 is an Alzheimer's Disease case that was not analysed for this thesis. **A.** Gel containing protein samples from patients with ID 82, 95, 105, and 122. **B.** Gel containing protein samples from patients with ID 122, 124, and 136

Table S1. Gene names of proteins identified in each sample at 1.5-100 fold in 5 positively labeled samples associated with tauopathies, including PSP, with the AR.

P1 (ID 82)	AR		AR		AR	P2 (ID 95)	AR		AR
C3	100	LYZ	100	NPTX1	1.977	C3	100	SYP	3.752
NRGN	100	RAB14	100	CLU	1.955	NRGN	100	TUBA4A	3.535
APOL2	100	RTN4[+]	100	PARK7	1.916	SELENBP1	100	SPTAN1[+]	2.850
SELENBP1	100	APLP2	100	SNCA	1.868	ACLY	100	PCSK1N[+]	2.383
AMPH	100	GAP43	5.136	IGSF8	1.810	PACSIN1[+]	100	DPYSL2	2.375
GNG3[+]	100	PCSK1N[+]	4.575	HSPA5	1.801	L1CAM[+]	100	NNT	1.841
ACLY	100	MAP1B[+]	4.565	SNAP25[+]	1.650	PURA[+]	100	VCP	1.759
HNRNPA2B1	100	NRCAM[+]	3.976	CNTNAP1[+]	1.649	SNCA	100		
NNT	100	THY1	3.429	CREBBP[+]	1.639	PRDX6	100		
ATP6V1G2	100	CNTN1[+]	2.760	PIP[+]	1.595	RACK1	100		
IGHG1	100	VCP	2.629	ADAM22[+]	1.594	PPP3CA	100		
L1CAM[+]	100	PRNP	2.535			PTRPRZ1	100		

CRYAB[+]	100	VAMP2+	2.146	TUBB2A	100		
PURA[+]	100	APOD	2.000	APOC3	100		

P3 (ID 105)	AR		AR	P4 (ID 122)	AR		AR
TUBB3	100	CNTN2[+]	100	ACLY	100	HSPA9	2.92
CKB[+]	100	CREBBP	14.844	APOC3	100	MAPK1[+]	2.881
MAP2	100	VCP	11.607	GNG3[+]	100	TUBB4A	2.79
CNTNAP1[+]	100	GAP43	4.163	EIF2S1	100	TUBA4A	2.477
SNCA	100	THY1	3.858	LYZ	100	GFAP	2.399
PURA[+]	100	NRCAM[+]	2.848	NRGN	100	TUBA1A	2.395
MAP1B[+]	100	GDI1[+]	2.393	MAP1B[+]	100	MAG	2.385
EPB41L3[+]	100	L1CAM[+]	2.322	PARK7	100	SPTAN1[+]	2.381
PLCB1[+]	100	C3	2.239	PDIA3	100	NAPB[+]	2.234
NAPB[+]	100	TUBB	2.225	PRNP	100	PPP3CA	2.223
APOC3	100	IGSF8	2.070	PTGDS	100	ATP1B1	2.153
HNRNPA2B1	100	CLU	2.020	RAB14	100	GAP43	2.099
MAG	100	CNTN1[+]	1.909	RACK1	100	CNP	2.058
AMPH	100	ATP5F1A	1.895	SOD2	100	STXBP1	2.025
SH3GL1	100	VAMP2[+]	1.825	VDAC1	100	NEFH	2.011
SLC1A3	100	VDAC1	1.818	SV2B[+]	100	EPB41L3[+]	1.968
PRNP	100	TUBA1A	1.594	ATP2A2[+]	100	DPYSL2	1.950
SOD2	100	CAMK2A	1.587	SH3GL1[+]	8.925	APOD	1.828
NRGN	100	PIP[+]	1.554	L1CAM[+]	6.973	CANX	1.689
PARK7	100	SPTAN1[+]	1.540	CRYAB[+]	6.588	PTPRZ1	1.678
ADAM22[+]	100	DPYSL2	1.500	TUBB	5.405	ACTB	1.671
RACK1	100			APOL2	5.077	S100A9	1.630
APLP2	100			MAP2	4.903	GDI1[+]	1.628
				IGHG1	4.662	VIM	1.610
				DECR1[+]	4.108	NPTX1	1.584
				CAMK2A	3.823	CKB[+]	1.578
				TUBB3	3.807	CNTNAP1[+]	1.571
				PLCB1[+]	3.612	ALB	1.570
				NEFL	3.513	RTN4[+]	1.559
				NRCAM[+]	3.145	SYN1[+]	1.542
				IGKC	3.1	VCP	1.533
				SCARB2[+]	3.040		

P5 (ID 136)	AR		AR		AR		AR
ANXA5[+]	100	CNTN2[+]	100	SV2A	4.232	GFAP	2.697
AMPH	100	UCHL1	100	APOD	3.886	ATP5F1A	2.660
PTGDS	100	HNRNPA2B1	100	GAP43	3.846	CAMK2A	2.648
EIF2S1	100	GPM6B[+]	100	ATP1A1	3.823	HSPD1	2.445
GNG3[+]	100	NNT	100	TUBB3	3.770	ACTB	2.403
MAP1B[+]	100	NAPB[+]	6.776	TUBB4A	3.694	TXN	2.385
PRNP	100	MAP2	6.363	CNTN1[+]	3.682	TUBA1A	2.276
SOD2	100	PPP3CA	6.138	CNP	3.601	CLU	2.218
PARK7	100	ARF5[+]	6.104	CANX	3.487	TUBA4A	2.171
RACK1	100	VAMP2[+]	5.869	DPYSL2	3.333	IGKC	2.015
VDAC1	100	ADAM22[+]	5.629	STXBP1	3.310	IGHG1	1.937
ACLY	100	NRCAM[+]	5.410	VIM	3.288	ATP1A2	1.910
SH3GL1[+]	100	SNAP25[+]	5.406	GDI1[+]	3.253	PTPRZ1	1.902
DECR1[+]	100	ATP6V1G2	5.361	NEFL	3.226	GAPDH	1.874
PLCB1[+]	100	GNAO1[+]	5.338	ATP1B1	3.001	SPTAN1[+]	1.714
MAPK1[+]	100	TUBB2A	5.085	MT3	2.991	SNCA	1.661
EPB41L3[+]	100	SYNJ1	4.648	APOC3	2.910	L1CAM[+]	1.659
CNTNAP1[+]	100	MOG	4.447	ATP1A3	2.749		
VCP	100	TUBB4B	4.250	HSPA5	2.708		

[+] Proteins included when 'include disease/phenotype association' is checked in IPA BioProfiler

Table S2. Gene names of proteins identified in each sample with (AR)>1.5-100-fold in positively labeled samples associated with neurodegeneration. AR is determined as abundance between patient and control samples. ID numbers refer to the unique identifier for each donor in the South Australian Brain Bank.

Patient 1 (ID 82)	AR	Patient 2 (ID 95)	AR	Patient 3 (ID 105)	AR		AR
C3	100	C3 100	100	SNCA	100	SOD2	100
FBXO2	100	SNCA 100	100	FTL	100	PARK7	100
FTL	2.681	SPTAN1 2.850	2.850	MAG	100	CREBBP	14.844
PRNP	2.535	DPYSL2 2.375	2.375	SH3GL1	100	C3	2.239
CLU	1.955	FBXO2 2.202	2.202	SLC1A3	100	CLU	2.020
PARK7	1.916			FBXO2	100	SPTAN1	
SNCA	1.868			PRNP	100	DPYSL2	
SNAP25	1.650						
CREBBP	1.639						

Patient 4 (ID 122)	AR		AR	Patient 5 (ID 136)	AR		AR
FTL	100	STXBP1	2.025	PRNP	100	VIM	3.288
PRNP	100	NEFH	2.011	SOD2	100	ATP1B1	3.001
SOD2	100	DPYSL2	1.950	PARK7	100	GFAP	2.697
PARK7	100	VIM	1.610	SH3GL1	100	RAB1A	2.682
SH3GL1	8.925			UCHL1	100	CLU	2.218
SCARB2	3.040			GPM6B	100	GAPDH	1.874
GFAP	2.399			SNAP25	5.406	FBXO2	1.773
MAG	2.385			SNCB	5.400	SPTAN1	1.714
SPTAN1	2.381			CNP	3.601	SNCA	1.661
ATP1B1	2.153			DPYSL2	3.333		
CNP	2.058			STXBP1	3.310		

[+] Proteins included when 'include disease/phenotype association' is checked in IPA BioProfiler

CHAPTER 4   Biotinylation by Antibody Recognition to identify proteomic constituents of TDP-43 inclusions in patient-derived fibroblasts: Amyotrophic Lateral Sclerosis

Article II   Establishing a Proximity-Ligation Method to Understand the Interactome of TDP-43 Aggregates in Amyotrophic Lateral Sclerosis

This article has been prepared for journal submission at the time of thesis submission

Chapter Introduction

Various proximity-ligation techniques for cell culture have been established, such as BioID and APEX. However, establishing a proximity-ligation method that can be used on both tissue and cells enables consistency across different material studied (e.g. tissue and cell culture) of the same disease. The BAR technique has been optimized for cell culture use in this chapter by initial work-up in HEK293 cells, which was then translated to experiments using patient fibroblasts. This addresses the rest of aim 1 in this thesis.

To be able to study ALS pathology in patient fibroblasts, they first need to be stressed to develop a consistent and inducible pathological response resembling the pathological inclusions that occur in motor neurons in patients i.e. cytoplasmic aggregation of pathological TDP-43. To do this, various concentrations of MG132 and sodium arsenite were tested to identify the best stressor to stimulate this pathology in cultured fibroblasts. Bringing about pathology in these cells could also be used clinically for diagnostic purposes. Limitations of working with fibroblasts are described in the article and include the fact that they are non-neuronal cells, however, the benefits are significant.

To address aim 3 of characterizing TDP-43 aggregates, a mass spectrometry workflow was implemented. Optimization of BAR in cell culture was conducted and implemented, followed with validation through confocal imaging and immunoblotting. Samples were gel purified before being processed through MS and the identified proteins lists were filtered and analysed with PD 2.4 and IPA. This is a proof-of-concept study that shows promising results for future investigation, as outlined in the article.

Contributions

Method	Contributors	Specific Contributions
BAR optimization	RR, PS, SR	RR optimized the BAR protocol for tissue, which was used for reference. PS undertook additional

		optimization for biotin cleavage, DAPI staining and optimizing for cell culture with the help and supervision of SR.
BAR labeling	PS	All.
Confocal imaging	RR	All.
Immunoblotting	PS, SR	Primarily undertaken by PS under supervision and training of SR.
Mass spectrometry	PS, SR, FC	PS and SR prepared the samples for mass spectrometry analysis. FC ran the samples through the mass spectrometer and uploaded raw data to Proteome Discoverer 2.4.
Data analysis	PS, SR, AL, RC	Primarily undertaken by PS, with guidance and training from SR, AL and RC.
Manuscript write-up	PS, RC	Written by PS with the intellectual guidance of RC.

Establishing a Proximity-Ligation Method to Understand the Interactome of TDP-43 Aggregates in Amyotrophic Lateral Sclerosis

Paulina Szwaja[1], Rowan Radford[1], Stephanie Rayner[1], Albert Lee[1], Flora Cheng[1], Roger Chung[1]

[1]Department of Biomedical Sciences, Faculty of Medicine, Health and Human Sciences, Macquarie University

Correspondence

paulina.szwaja@hdr.mq.edu.au

Abstract

Amyotrophic lateral sclerosis (ALS) is a progressive neurodegenerative disease pathologically characterized by insoluble TDP-43 inclusions in motor neurons. Understanding the protein interactome of these inclusions may uncover important insight into the pathological mechanisms of ALS. Typical proximity-ligation methods require a fusion protein and may result in non-specific binding. Thus to limit these problems, an unbiased proteomic approach was taken to label co-aggregating proteins within fibroblasts derived from healthy and ALS-afflicted patients. This approach, termed biotinylation by antibody recognition (BAR), is a recently described method that makes use of a primary antibody binding to the protein of interest (POI) and, with the addition of a secondary antibody conjugated to horseradish peroxidase, hydrogen peroxide and biotin tyramide, facilitates biotinylation of proteins proximal to the POI. Then the proteins are biochemically isolated and identified using mass spectrometry. With this workflow and bioinformatic analysis, several proteins known to interact with TDP-43 directly and indirectly have been identified along with potentially novel interactors. The data here substantiates this unbiased approach of rapidly labeling and identifying components of aggregates within cultured cells with a broad application to other diseases and interaction studies.

Key words: Amyotrophic lateral sclerosis; TDP-43 pathology, biotinylation, neurodegeneration, proximity ligation, mass spectrometry

Introduction

Amyotrophic lateral sclerosis (ALS) is a progressive degenerative disease of the upper and lower motor neurons in the cerebral cortex and spinal cord respectively. ALS is characterized by muscular weakness and dystrophy, with eventual respiratory failure being the cause of death 3-5 years after diagnosis [19, 35]. Riluzole [7, 26] and edaravone [12, 24] are part of the few available treatments currently, which aim to treat symptoms. The majority of cases are sporadic (90%) with the other 10% due to familial inheritance of certain gene mutations [29]. Regardless of whether the disease is sporadic or familial in origin, all cases are indistinguishable on a clinical and molecular level [29]. Although there is a significant lack of understanding of disease pathogenesis in all cases, we understand the pathological hallmark to be aggregation of proteins in the cytoplasm of motor neurons [10]. In 97% of cases, the hyperphosphorylated and ubiquitinated transactive response DNA-binding protein 43kDa (TDP-43) is the aggregating protein, encoded by the *TARDBP* gene [21, 29, 32]. TDP-43 is typically located within the nucleus of healthy cells, but in ALS it mislocalizes into the cytoplasm where it aggregates to form insoluble inclusions [21]. Notably, mutations in *TARDBP* make up only 5% of familial cases [32], which suggests a dysfunction within TDP-43 in particular, or proteins that interact with TDP-43 directly or indirectly, such as RNA-binding proteins and nucleocytoplasmic transporter proteins, are crucial disease-modifiers that influence the pathogenesis of ALS.

Protein-protein interactions (PPIs) have been studied in various ways, from biochemical extraction to affinity purification and proximity-ligation methods in recent years [6, 13-14, 18, 20, 25, 27-28]. Around 50 years ago, affinity chromatography was developed to separate POIs from complex mixtures with reliance on highly specific interactions, such as antibody-to-antigen binding [6]. This method has been improved upon over the years to improve reliability. A challenge with chromatography-based separation techniques include over-loading with sample (which can clog the column), very long collection and flushing times, and difficult to control peak elution [2, 5, 27]. Over the years, this purification technique has been optimized by using magnetic beads, allowing easy "recapture" of the beads and therefore allows limitless sample loading and washing, thus becoming a popular and conventional method for protein interaction studies still used today. However, this method of protein extraction comes with notable shortcomings, including low abundance proteins being difficult to detect, nor can insoluble proteins or proteins with weak or transient interactions be easily captured. However, immunoprecipitation (IP) is still used in combination with newer

methods. To address IP limitations, proximity-ligation methods were developed [18, 25, 27].

Proximity ligation assays were first described in 2002 by Fredriksson and colleagues [8], soon after becoming commercialized, established, and generally applicable for protein analysis, including protein-protein interactions (PPIs) with high specificity and sensitivity. This is especially important when looking at large protein samples to sample loss in the process. The overarching benefit of recent proximity-ligation methods is the use of biotin-mediated isolation of proteins as biotinylation is chemically resistant to harsh lysis buffers such as SDS, radioimmunoprecipitation assay (RIPA) buffer and urea that are required to solubilize insoluble pathological protein aggregates [16, 31]. The reason for this is that the binding of biotin and streptavidin is very strong and specific. The proximity ligation method was improved upon over the years to yield BioID [28] and BioID2 [13], which incorporates a smaller biotin ligase, shorter biotinylation time and less biotin needed for maximum biotinylation (Fig. 1). Additionally, flexible linkers have been added to increase the amount of proteins able to be captured on the streptavidin bead (Fig. 2). However, these studies are limited to live cells and involve a long biotinylation time. To overcome such limitations, biotinylation by antibody recognition was devised in 2018.
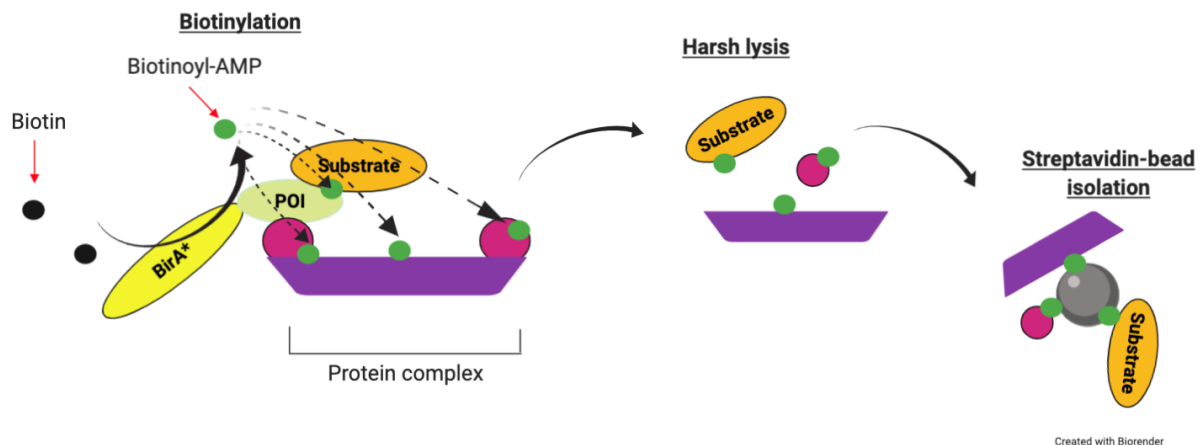

Fig. 1 The biotinylation process and extraction of biotinylated proteins by BioID/2. Created with biorender.com
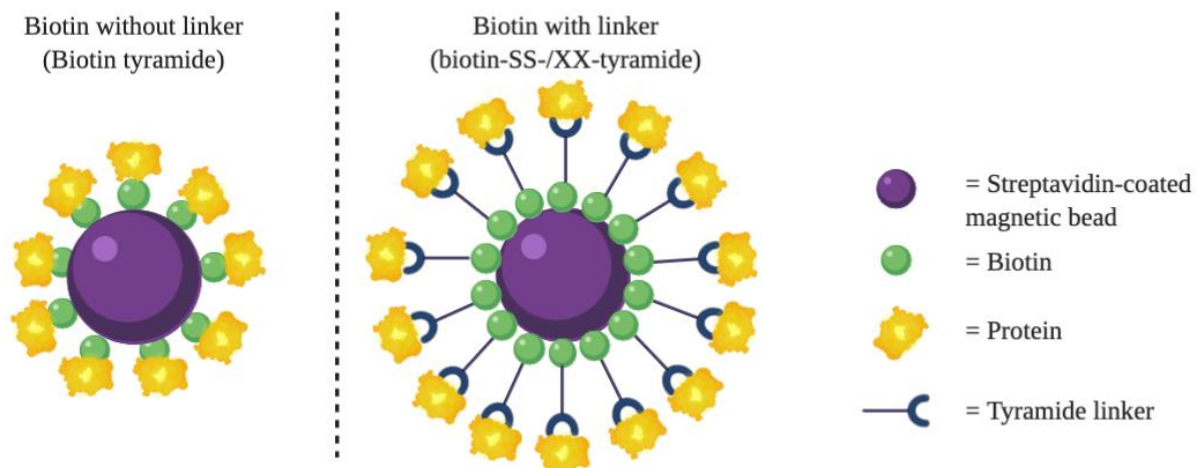
Fig. 2 Representation of biotin tyramide with and without linkers capturing proteins. **A.** Shows crowding of biotinylated proteins on a small surface, limiting how many proteins can be captured. **B.** Shows biotinylated proteins with a linker, increasing the surface area of protein capture. Created with biorender.com

Biotinylation by antibody recognition (BAR) is a recently developed proximity-ligation method for use on fixed tissue and cells, which is well suited for protein aggregation studies [2]. After sample fixation, a primary antibody is used to recognize the POI. Then, a secondary antibody conjugated to horseradish peroxidase is attached to the primary antibody, which facilitates rapid biotinylation of proteins proximal to the POI in the presence of hydrogen peroxide and biotin phenol (Fig. 3). A flexible biotin tyramide linker is used to biotinylate more proximal proteins than regular biotin-tyramide. This approach in cell culture can save a lot of time in biotinylation compared to BioID and allows the study of aggregates directly without a fusion protein that may alter protein function and, therefore, the results.
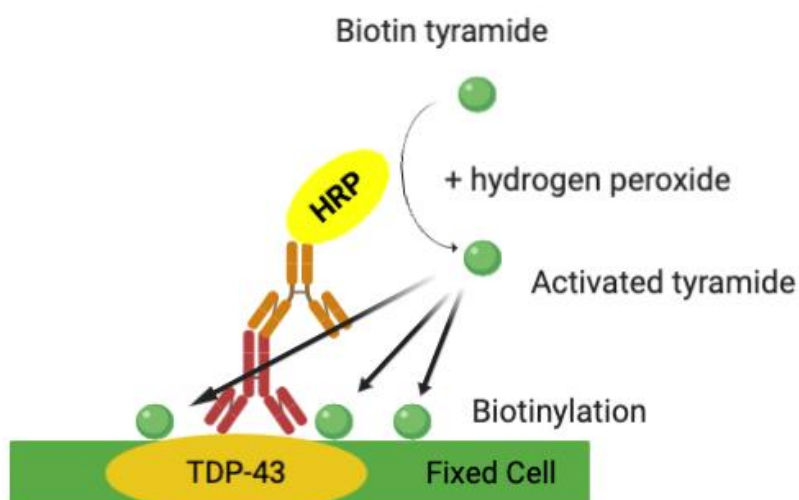
Fig. 3 The BAR labeling process at the molecular level. Created with biorender.com

This study reports the first use of BAR to characterize the interactome of TDP-43 in response to cellular stressors in fibroblasts taken from ALS patients. The main aims of this work is to optimize the BAR technique to cell culture and characterize TDP-43 aggregates within fibroblasts of ALS patients. This project employs the use of a mass spectrometer to identify proteins isolated from the complex samples using BAR with a workflow provided in Fig. 4.
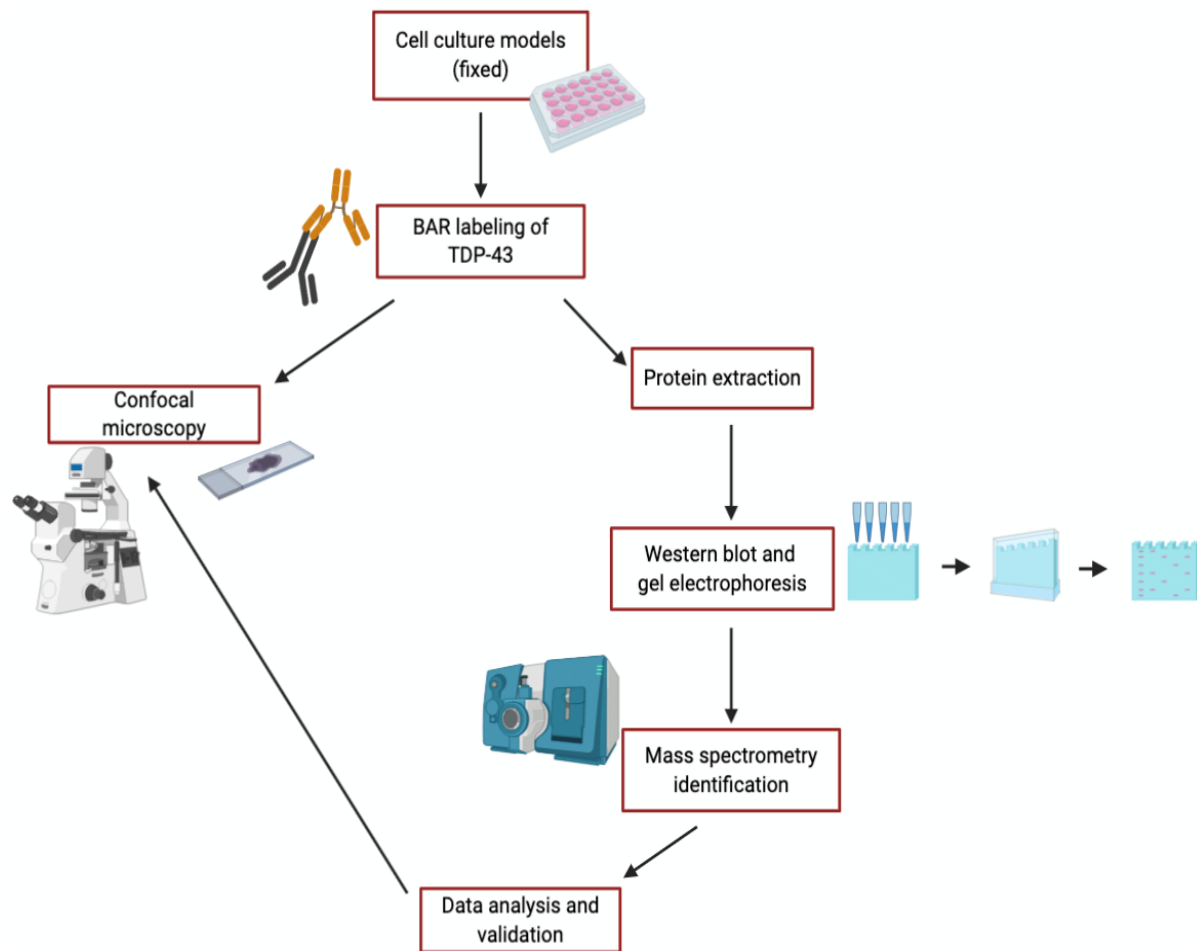
Fig. 4 The BAR-MS workflow for this project. Created with biorender.com

Materials and Methods

Cell culture

Human patient fibroblast cells were used for this project. The fibroblasts were collected from ALS patients at Macquarie University, under the approval of Macquarie University Neurodegenerative Diseases Biobank (5201600387). Fibroblasts were initially grown in T25 flasks before being transferred into T75 flasks in Dulbecco's Modified Eagle Medium

(DMEM) with 20% heat-inactivated foetal bovine serum (FBS), incubated at 37℃ with 5% CO_2 and 95% humidity. Cells were grown to ~80% confluency before subculture.

For subculture, the media was aspirated and the cells were washed with phosphate buffered saline (PBS). Trypsin was used to detach cells from the flask before being split into two new T75 flasks or a 24-well plate. Reagents used for cell culture are summarized in table 1.

Table 1 Reagents used in study

Reagents	Catalogue/Company	Concentration
Normal Goat Serum	G9023/Sigma-Aldrich	1% and 10% (v/v)
Biotin-XX-tyramide SuperBoost™ Kit	B40911/ Invitrogen	N/A
Biotin-SS-Tyramide	LS-3570.0250/Iris Biotech	50nM
DAPI	D1306/Life Technologies	3 µM
Prolong™ Glass	P36984/Life Technologies	N/A
TDP-43 Rabbit Polyclonal antibody	10782-3-AP/ProteinTech	1:500
Goat anti-rabbit Alexa Fluor® 488	A11008/Invitrogen	1:1000
Goat anti-rabbit Alexa Fluor® 647	ab150087/Abcam	1:1000

Drug treatments

At 80% confluence, fibroblasts (table 2) were seeded into 100mm plates of 4 biological replicates at a density of 1×10^5 cells/mL and left to grow to 80% confluence again at 37℃. The oxidative stressor sodium arsenite (SA) was added to 2 plates at a concentration of 500µM for 1 hour along with 2 water control plates at 37℃ before cells were fixed with 4% paraformaldehyde.

Table 2 Fibroblasts provided by the genetics team at the MND research centre, Macquarie University

Fibroblast type	Sample ID	Sample source	Note	Used in final data collection
Control	MQPS15001	Macquarie Plastic and Reconstructive Surgery	Healthy	Yes
Control	MQPS170001	Macquarie Plastic and Reconstructive Surgery	Healthy	Yes
Control	MQPS16001	Macquarie Plastic and Reconstructive	Healthy	No

		Surgery		
CCNF patient	ANZAC170057	ANZAC Research Institute	CCNF patient with S621G mutation, Collected in 2017	No
CCNF patient	ANZAC160077	ANZAC Research Institute	CCNF patient with S621G mutation, Collected in 2016	No
CCNF patient	23032	ANZAC Research Institute	CCNF patient with S621G mutation, Collected in 2013	Yes
CCNF carrier	19006	ANZAC Research Institute	CCNF pre-symptomatic case with S621G mutation, collected in 2013	Yes

BAR labeling

Fibroblasts

To determine conditions that would induce TDP-43 translocation and aggregation in patient-derived fibroblasts, healthy control and ALS mutant fibroblasts were treated with either 500µM SA or a vehicle (water) control. Each experimental condition was repeated 2 times per patient cell line. Cells were permeabilized using 0.1% triton X-100 in PBS before being blocked with 1% bovine serum albumin (BSA) in glycine (Sigma-Alrich) and PBST for 30mins. Primary antibody against TDP-43 (rabbit; ProteinTech) was diluted 1:500 and incubated overnight at 4°C in the appropriate samples in 1 SA treated sample and 1 vehicle (veh) control sample per patient cell line. Goat conjugated superboost HRP (anti-rabbit) was added for 1 hour at room temperature (RT) before being washed with PBST and the solution replaced with 100nM of biotin-SS-tyramide in H_2O_2 and blocking buffer made from the Superboost Kit (Thermo Scientific) for up to 5mins. The reaction was stopped using 500mM sodium ascorbate (Sigma-Aldrich) for 5mins and the cells were washed with PBST. The cells were then scraped from the plates and transferred into 1.5mL Eppendorf tubes ready for aggregate isolation

Confocal Imaging

Fluorescent streptavidin 647N (1:400) and secondary antibody (Alexa Fluor 488 goat anti-mouse 1:250) were added to sections overnight at 4°C before counterstaining the next day with 3µM DAPI in TBS for 2 hours at RT. The sections were washed and mounted onto glass slides using ProLong$^{\text{TM}}$ Glass Antifade mountant (Invitrogen). Widefield fluorescence microscopy was conducted on the Leica SP5x with resonant scanner confocal microscope.

Western Blot Analysis

Protein concentrations were determined with a Pierce™ BCA Protein assay kit. Equal protein amounts were aliquoted into the wells of 4-15% gradient SDS-PAGE gels (Invitrogen) in 1X loading buffer and separated by electrophoresis. Proteins were transferred onto a nitrocellulose membrane using the Trans-blot Turbo transfer system (Bio-Rad). Then, membranes were blocked for 30 min in Odyssey blocking buffer at RT. The membrane was then incubated in streptavidin conjugated to a fluorophore, diluted 1:1000 in the blocking buffer. Images were taken using the Li-Cor Odyssey CLx Imaging System, and the images were analysed with Image Studio Software.

Isolation of biotinylated proteins

Biotinylated fibroblasts were scraped into separate tubes twice in BAR lysis buffer (total 750µL). The cells were then probe-sonicated at 40% power and 30% pulser 15 times before being reverse cross-linked in 95°C for 1 hour and 60°C for 2 hours. The samples were cooled to 4°C before adding 1X protease inhibitor cocktail (Roche) and centrifuged at 1000 rcf at 4°C for 5 min. The samples were quantified using the bicinchoninic acid assay (BCA) kit.

Equal amounts of protein were aliquoted and streptavidin-coated magnetic beads (Pierce™) were washed with RIPA lysis buffer before 10uL was added to each sample. The samples were left on a rotating rack overnight at 4°C. Magnetic beads with the biotinylated proteins were isolated on a magnetic rack, and to reduce non-specific binding, these beads were washed twice with RIPA lysis buffer (1% NP-40, 0.1% SDS, 50mM Tris HCl, 150mM NaCl, 0.5% Sodium Deoxycholate, 1mM EDTA and 0.01% sodium azide, pH of 7.4), once with 1M KCl, 1M Na_2CO_3, 2M urea buffer (2M urea, 10mM Tris-HCl), and finally twice with RIPA buffer.

Mass Spectrometry Preparation

In-gel trypsin digest

The biotinylated proteins were cleaved from the streptavidin beads using 100mM dithiothreitol (DTT) (Invitrogen). The samples were then loaded into a 4%-12% Bis-Tris NuPAGE 10 well protein gel (Invitrogen). The gels were run for 5 min at 180V before the gels were taken out and left in Coomassie stain (Thermo Scientific) for 1-2 hours (until banding was seen). The gels were then de-stained in 25% methanol, with 2 solution changes over the first 2 hours, the left in fresh de-stain solution overnight. The gels were imaged

using LiCor Odyssey CLx before the samples were cut from the gels into 1mm cubes and transferred into v-bottomed 96-well plates (Corning®). The gels were further destained until Coomassie blue banding was barely visible, then incubated in 10mM DTT in 50mM AmBic (ammonium bicarbonate) at 37°C for 40 min. Then the samples were alkylated with 20mM IAA (Sigma-Aldrich) in 50mM AmBic for 40 min at room temperature in the dark. Once the samples were dry, 10µg/mL of sequencing grade trypsin in 50mM AmBic was added to each and were incubated overnight at 37°C. The resulting peptides were transferred to new tubes and lyophilized in a Speedvac.

Sample purification

C18 OMIX tips (Agilent) were pre-washed and equilibrated to desalt peptides once suspended in 0.1% formic acid (FA). The peptides were lyophilized again in a Speedvac before being prepared for MS analysis.

Mass Spectrometry

The lyophilized peptides were again resuspended in 0.1% FA and centrifuged at 14,000 rcf for 15 minutes to remove insoluble debris. The clarified peptides were added to glass vials and analysed by LC-MS/MS. Peptides were separated with the Ultimate 2000 nanoLC (Thermo Scientific) fitted with an Acclaim PepMap RSLC column (Thermo Scientific) on a 120 minute gradient with a flow rate of 300nL/min (2-95% v/v AcN, 0.1% v/v FA). Eluted peptides from nano LC column were ionized into the Q Exactive Plus mass spectrometer (Thermo Scientific). A 10µm emitter tip was fitted to the electrospray source with the electrospray voltage maintained at 1.5kV (New Objective, Woburn, MA). The capillary temperature was set to 25°C. The precursor ions for MS/MS fragmentation were selected using a data-dependent "top 15" method running in FT-FT acquisition mode with HCD fragmentation. The FT-MS analysis was performed at 70,000 resolution and a $1x10^6$ ions AGC target in full MS. MS/MS scans were performed at 35,500 resolution and a $2x10^5$ ions AGC target. Injection times were set to a maximum of 121 milliseconds. For triggering MS/MS fragmentation, the ion selection threshold was set to 25,000 counts, and a 1.4 m/z isolation width and normalized collision energy of 27 were employed to perform HCD fragmentation.

Bioinformatics and Statistics

The MS data obtained from the fibroblast samples were first analysed in Proteome Discoverer (PD) 2.4 (Thermo Scientific). The peptides were searched against the *Homo sapiens* SwissProt database with the following parameters. Trypsin as the enzyme, with a maximum of three missed cleavage sites allowed. The precursor mass tolerance was set to 20ppm and fragment mass tolerance set to 0.1 Da. The maximum equal modification was set at three per peptide, with dynamic modifications set to oxidation of methionine, biotinylation of K and N-terminus of protein, and acetylation of N-terminus. The static modification used was carbamidomethylation modification of cysteine, and normalization was set to none. Data was further process in a Label-Free Quantitation (LFQ) workflow using the Minora Feature node and percolator node. The latter node estimates false discovery rates at the protein level through an incorporated decoy database. Additionally, the percolator node was used for FDR estimations at the peptide-to-spectrum matches (PSMs) level. Results were adjusted for final global FDR to be less than 1% at both peptide and protein levels, and proteins were listed if 2 or more unique peptides were identified. A requirement for validation of protein identifications was a q-value <0.01.

The data generated here was exported into Microsoft Excel, where the data was further filtered using abundance ratios that had a fold change of >1.5 and <0.5. This data was then input to Ingenuity pathway analysis (IPA) (QIAGEN) to characterize and classify the identified proteins and their interaction partners according to molecular function. For this, a right-tailed Fischer's Exact Test was used. Statistically significant results were considered to be at a p-value ≤ 0.05.

Results

Optimization of Drug Treatment for Fibroblasts

Patient-derived fibroblasts were used to optimize drug treatment concentrations for the formation of TDP-43 aggregates and mislocalization of TDP-43 into the cytoplasm. Initial starting concentrations were determined based on previous papers in cultured cells with additional concentrations for comparison. MG132 was tested at 5µM, 10µM, 15µM and 20uM. Sodium arsenite was tested at 0.5mM, 1mM, 1.5mM and 2mM. The primary antibodies used to observe pathological change were against TDP-43 and FK2 (ubiquitin) (Enzo). Although MG132 treatment produced some more TDP-43 and ubiquitin in the

fibroblasts compared to negative controls, there was no observable difference between all the MG132 concentrations (Fig. 4a), as well as no noticeable pathology was formed (either inclusions or cytoplasmic mislocalization of TDP-43). SA was observed to be optimal at 0.5mM, with high cell death occurring at higher concentrations. TDP-43 and ubiquitin were observed at much higher concentrations than MG132 (Fig. 4b). The incubation time of the S.A. treatment at 3 hours, as done by Yang et al. [36], was reduced to 1 hour to decrease mass cell death observed, and then the samples were fixed, labeled and processed for MS as described above. Mislocalization of TDP-43 into the cytoplasm was observed in disease patient cells treated with SA, while none was observed in healthy patient cells treated with SA. Reduction of SA treatment to 1 hour still induced observable TDP-43 mislocalization in patient cells.
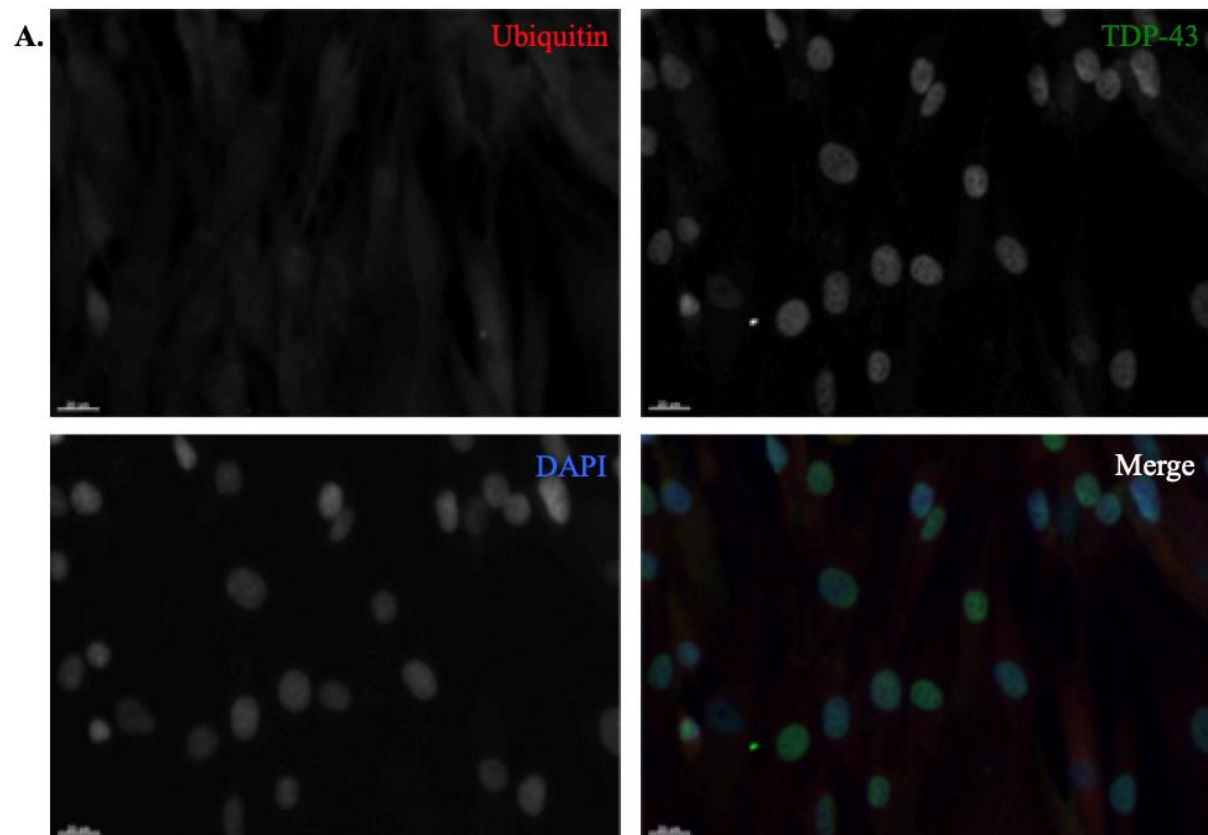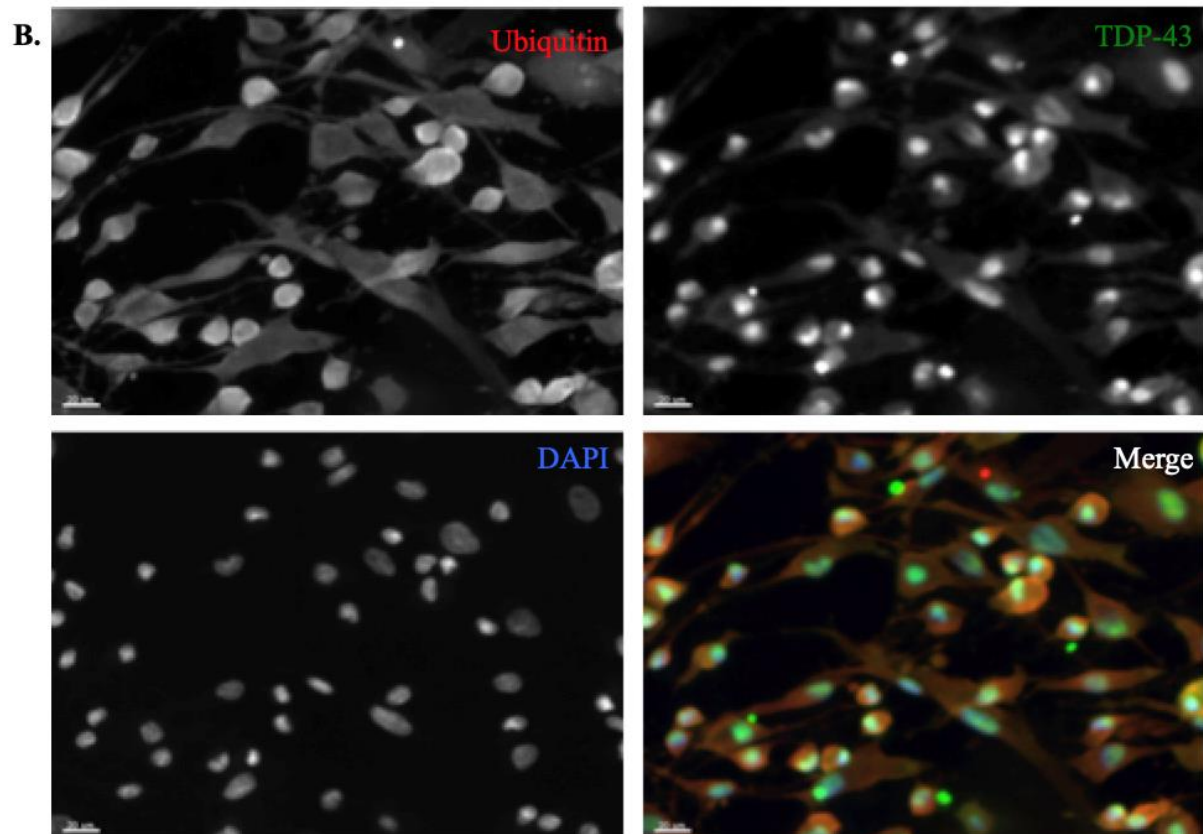
Fig. 4 Representative images of fibroblasts with the S621G mutation (patient 23032) treated with cell stressors. **A.** Fibroblasts treated with 1.5μM MG132 for 1h. **B.** Fibroblasts treated with 0.5mM SA for 3h. Image brightness and contrast was normalized (i.e. same conditions for image capture). Scale bars are 20μm

Characterizing TDP-43 aggregates in ALS fibroblasts

Following BAR labeling, fibroblasts were scraped into Eppendorf tubes and biotinylated proteins were isolated with streptavidin beads. These proteins were then cleaved off the beads using DTT and were separated using a 4-12% Bis-Tris NuPAGE gel before the gels were stained with Coomassie blue. Numerous protein bands were observed in the SA treated, BAR labeled samples whilst fewer bands were observed in the negative controls, demonstrating low background noise in the negative controls (Fig. S1). In total, 1244 proteins were identified in all samples generated through MS analysis, and IPA was used to characterize pathological TDP-43 aggregates in SA treated fibroblasts. The raw MS data was filtered through Microsoft Excel to include proteins with a standard abundance ratio (AR) of 1.5 to 100. The proteins were further filtered using Bioprofiler in IPA to generate a list of proteins known to be involved in ALS pathology. These proteins were assessed against the raw data to determine the efficacy of this filtering method. Additionally, proteins were filtered to identify those involved in neurodegeneration. All the proteins are listed in tables 3–6. These final

protein lists provide insight into the altered TDP-43 interactome that occurs during stress in healthy and ALS patients.

Table 3 A comparison of proteomic profiles of TDP-43 inclusions in fibroblasts compared between WT SA and WT veh conditions, with proteins that show up in Bioprofiler (IPA) under ALS related proteins and neurodegeneration related proteins

ALS	AR	Neurodegeneration	AR
BCL-2-like protein 4	100	C-type natriuretic peptide	100
Mitogen-activated protein kinase 1	100	Fibroblast growth factor 2	3.638
Phosphoribulokinase	100	Protein-glutamine gamma-glutamyltransferase 2	2.429
S100 calcium-binding protein A4	2.645	Ubiquitin carboxyl-terminal hydrolase isozyme L1	2.354
Annexin A1	2.119	Endophilin-A2	2.203
Reticulon-4	-100	Laminin subunit gamma-1	-2.506
TDP-43	-100	VPS35 endosomal protein sorting factor-like	-2.611
		Peroxisomal membrane protein PEX13	-5.128
		Phosopholipid hydroperoxide glutathione peroxidase	-100
		Prolow-density lipoprotein receptor-related protein 1	-100
		Protein NDRG1	-100

Table 4 A comparison of proteomic profiles of TDP-43 inclusions in fibroblasts compared between S621G veh and WT veh conditions, with proteins that show up in Bioprofiler (IPA) under ALS related proteins and neurodegeneration related proteins

ALS	AR		AR	Neurodegeneration	AR
Annexin A11	100	Collagen alpha-2(I) chain	2.654	Signal transducer and activator of transcription 3	100
Melanoma-associated antigen D1	100	Tubulin alpha-4A chain	2.595	Laminin subunit gamma-1	100
Mitogen-activated protein kinase 1	100	Elongation factor 1-alpha 1	2.386	Stathmin	100
Melanoma-associated antigen D2	21.811	Fatty acid synthase	2.34	26S proteasome regulatory subunit 4	100

Protein	Value	Protein	Value	Protein	Value
S100 calcium-binding protein A4	6.285	Sequestosome-1	2.151	Dihydropyrimidinase-related protein 3	100
Dynactin subunit 1	6.278	Eukaryotic initiation factor 4A-I	2.06	C-type natriuretic peptide	100
Heterogeneous nuclear ribonucleoprotein A1	5.643	Neurofilament light polypeptide	-2.681	Signal transducer and activator of transcription 1-alpha/beta	4.227
TDP-43	4.687	Reticulon-4	3.69	Spectrin alpha chain, non-erythrocytic 1	3.845
Transitional endoplasmic reticulum ATPase	3.345	S100 calcium-binding protein A6 -4.367	-4.367	Cytoplasmic dynein 1 heavy chain 1	3.037
Optineurin	3.291	Nicotinamide N-methyltransferase	-12.048	Protein-glutamine gamma-glutamyltransferase 2	2.845
Transmembrane glycoprotein NMB	3.102	Clusterin	-100	Mitochondrial antiviral-signaling protein	2.391
Annexin A1	3.093	Collagen-alpha 1(III) chain	-100	Lamin-B1	2.337
T-complex protein 1 subunit beta	3.043	Transferrin receptor protein 1	-100	Phospholipid hydroperoxide glutathione peroxidase	-2.874
				Prolow-density lipoprotein receptor-related protein 1	-8.130
				Protein NDRG1	-100
				Glutathione peroxidase-like peroxiredoxin gpx1	-100
				Ubiquitin carboxyl-terminal hydrolase isozyme L1	-100
				Serine/threonine-protein PINK1, mitochondrial	-100
				Peroxisomal membrane protein PEX13	-100

Table 5 A comparison of proteomic profiles of TDP-43 inclusions in fibroblasts compared between S621G SA and WT SA conditions, with proteins that show up in Bioprofiler (IPA) under ALS related proteins and neurodegeneration related proteins

ALS	AR	Neurodegeneration	AR
Annexin A11	100	Zinc finger protein ZPR1	100
Melanoma-associated antigen D1	100	Phosopholipid hydroperoxide glutathione peroxidase	100
TDP-43	100	Prolow-density lipoprotein receptor-related protein 1	100
Transmembrane glycoprotein NMB	9.837	Signal transducer and activator of transcription 3	100
Dynactin subunit 1	4.206	Laminin subunit gamma-1	100
Melanoma-associated antigen D2	3.48	Stathmin	100
Transitional endoplasmic reticulum ATPase	2.493	26S proteasome regulatory subunit 4	100
Matrin-3	2.419	Mitochondrial antiviral-signaling protein	5.331
Heterogeneous nuclear ribonucleoprotein A1	2.254	Caveolin-1	3.455
Actin, alpha cardiac muscle 1	-2.924	Lamin-B1	3.124
Neurofilament light polypeptide	-7.576	Edophilin-A2	2.960
Clusterin	-100	Signal transducer and activator of transcription 1-alpha/beta	2.277
Collagen-alpha 1(III) chain	-100	Dihydropyrimidinase-related protein 2	-2.033
Mitogen-activated protein kinase 1	-100	Protein-glutamine gamma-glutamyltransferase 2	-4.762
Nicotinamide N-methyltransferase	-100	Fibroblast growth factor 2	-100
Transferrin receptor protein 1	-100	Microtubule –associated protein 1A	-100
		Glutathione peroxidase-like peroxiredoxin gpx1	-100
		Ubiquitin carboxyl-terminal hydrolase isozyme L1	-100
		Serine/threonine-protein PINK1, mitochondrial	-100

Table 6 A comparison of proteomic profiles of TDP-43 inclusions in fibroblasts compared between S621G SA and S621G veh conditions, with proteins that show up in Bioprofiler (IPA) under ALS related proteins and neurodegeneration related proteins

ALS	AR	Neurodegeneration	AR
Collagen-alpha 1(III) chain	100	Zinc finger protein ZPR1	100
S100 calcium-binding protein A6	9.433	Peroxisomal membrane protein PEX13	100
BCL-2-like protein 4	-2.004	Syntaxin-binding protein 1	3.619
TDP-43	-2.141	Spectrin alpha chain, non-erythrocytic 1	-2.114
Matrin-3	-2.146	Signal transducer and activator of transcription 3	-2.740
S100 calcium-binding protein A4	-4.976	Prolow-density lipoprotein receptor-related protein 1	-2.915
Optineurin	-5.405		
Mitogen-activated protein kinase 1	-100		
Reticulon-4	-100		

Discussion

The BAR method enabled us to identify proteins closely associated with TDP-43 aggregation and nucleocytoplasmic mislocalization following stress-induced conditions in cultured human fibroblasts. This provides direct insight into some of the proteins that may be involved in the development of disease pathology in ALS patients. What is most interesting is the difference between WT and S621G samples. It should be noted that TDP-43 levels were observed to be consistent across all samples within each respective condition.

First, we analysed the proteins identified in the WT SA and WT vehicle-treated samples. The list includes a mixture of upregulated proteins in the WT SA sample that are involved in increased neurodegeneration and decreased neurodegeneration. This may suggest these proteins are involved in the stress response and try to bring the cell back to balance. TDP-43 was found solely in the WT vehicle control, which may signify the fact that TDP-43 became insoluble after oxidative stress and will need to be validated by analysing the insoluble fractions that were not analysed in this study.

In comparing the SA treated WT cells to SA treated S621G cells there is a clear difference in the proteins that appear and their relative fold change. Whereas in the WT SA condition many proteins involved in ALS are downregulated, they appear upregulated in the S621G SA

sample. This suggests the proteins' involvement in the stress response or role in neurotoxicity. Many of these proteins appear in the S621G vehicle-treated sample, which may imply that the mutation itself is what drives these proteins across to be drivers of pathology, but additional stress (i.e. SA treatment) would rapidly accelerate this damaging process. HnRNPA1 and matrin-3 are interesting (increased 2.254 and 2.149 fold respectively in association with TDP-43 when comparing S621G SA treated cell to WT, SA treated cell) as they are usually involved in stress-responses and form stress granules and paraspeckles respectively [9, 15, 22, 30]. They control gene regulation during the stress period by holding mRNA. Dynactin [17] is also interesting (increased 4.206 fold in association with TDP-43 when comparing S621G, SA treated cells to WT, SA treated cells) as it is involved in protein translocation and may play a role in TDP-43 translocation during oxidative stress from SA treatment. Furthermore, some proteins such as FGF2 [11, 34], that are associated with reduction of neurodegeneration, are upregulated in WT SA but not found in S621G SA. This further supports a dysregulation in the stress response in someone with ALS, leading to degeneration of motor neurons.

There are some clear limitations in taking this approach to analysing data in IPA as many proteins known to be associated with ALS did not appear with the selected parameters (such as other RNA binding proteins and heat shock proteins). A functional analysis of the proteins that do appear may absolve this issue as the molecular pathways affected will shed insight into the other proteins involved in the pathway that were isolated from the samples.

A limitation of using fibroblasts is that they are dividing cells and will therefore contain proteins that the non-dividing neuronal cells would lack. As a result, it is pertinent that the data obtained be looked to as a guide for future studies in primary neurons, such as induced pluripotent stem cells derived from patients. Another limitation is the number of patient cell lines we were able to use. Only one mutant and two healthy control cell lines were used in this study. This was due to the cells growing at different rates, with many not growing to 80% confluence in time for biotinylation and MS preparation, limited by the closure of PC2 laboratories due to COVID-19. However, all of the patient cells will be utilized in future experiments. Using patient fibroblasts serves a great purpose in studying ALS, as they are endogenous regulators of TDP-43. Other studies may often artificially overexpress TDP-43 in cells, however they are much easier to study, as there is more expression of TDP-43 [14].

Nevertheless, this proof of concept study illustrates promising results for further investigation and validation.

Additional studies are needed to identify and validate known and novel protein interaction partners using standard IHC approaches. Furthermore, more rigorous optimization in cell drug treatment is needed such as concentration and timing to produce a higher amount of pathological TDP-43 with minimal cell death, as well as increase sample amount used. In addition, it will be important to quantify how much TDP-43 is mislocalized in disease patient cells compared to healthy patient cells before and after SA treatment for better data interpretation. There is, however, concern of how much primary antibody will be used (i.e. the cost will be quite large). This may be rectified with optimization of the primary antibody labeling step in the BAR method. Moreover, various antibodies will be tested to assess which ones are optimal to answer different questions (i.e. antibodies that specifically bind to pathological, hyperphosphorylated TDP-43 compared against antibodies that bind to all TDP-43). The results from the patient-derived fibroblasts used here may be compared with fibroblasts containing other ALS-causing mutations. Overall, BAR is a promising method to further develop our insight into ALS pathology with a widespread application to other diseases.

References

1. Arai T, Nonaka T, Hasegawa M, Akiyama H, Yoshida M, Hashizume Y, Tsuchiya K, Oda T, Ikeda K (2003) Neuronal and glial inclusions in frontotemporal dementia with or without motor neuron disease are immunopositive for p62. Neuroscience Letters 342:41-44. doi:10.1016/S0304-3940(03)00216-7

2. Bar DZ, Atkatsh K, Tavarez U, Erdos MR, Gruenbaum Y, Collins FS (2017) Biotinylation by antibody recognition: a method for proximity labeling. Nature methods 15. doi:10.1038/nmeth.4533

3. Beere HM (2004) "The stress of dying": the role of heat shock proteins in the regulation of apoptosis. Journal of cell science 117:2641. doi:10.1242/jcs.01284

4. Blokhuis A, Groen E, Koppers M, Berg L, Pasterkamp R (2013) Protein aggregation in amyotrophic lateral sclerosis. Pathology and Mechanisms of Neurological Disease 125:777-794. doi:10.1007/s00401-013-1125-6

5. Chen C-L, Perrimon N (2017) Proximity-dependent labeling methods for proteomic profiling in living cells. Wiley Interdisciplinary Reviews 6. doi:10.1002/wdev.272

6. Cuatrecasas P, Wilchek M, Anfinsen CB (1968) Selective Enzyme Purification by Affinity Chromatography. Proceedings of the National Academy of Sciences of the United States of America 61:636-643. doi:10.1073/pnas.61.2.636

7. Fang T, Al Khleifat A, Meurgey J-H, Jones A, Leigh PN, Bensimon G, Al-Chalabi A (2018) Stage at which riluzole treatment prolongs survival in patients with amyotrophic lateral sclerosis: a retrospective analysis of data from a dose-ranging study. The Lancet Neurology 17:416-422. doi:10.1016/S1474-4422(18)30054-1

8. Fredriksson S, Gullberg M, Jarvius J, Olsson C, Pietras K, Gústafsdóttir SM, Östman A, Ulf L (2002) Protein detection using proximity-dependent DNA ligation assays. Nature biotechnology 20:473. doi:10.1038/nbt0502-473

9. Guil S, Long JC, Caceres JF (2006) hnRNP A1 Relocalization to the Stress Granules Reflects a Role in the Stress Response. Molecular and Cellular Biology 26:5744. doi:10.1128/MCB.00224-06

10. Heemels M-T. (2016) Neurodegenerative diseases. Nature 539:179.doi:10.1038/539179a

11. Henriques A, Pitzer C, Schneider A (2010) Neurotrophic growth factors for the treatment of amyotrophic lateral sclerosis: where do we stand? Frontiers in neuroscience 4:32-32. doi:10.3389/fnins.2010.00032

12. Ito H, Wate R, Zhang J, Ohnishi S, Kaneko S, Ito H, Nakano S, Kusaka H (2008)

Treatment with edaravone, initiated at symptom onset, slows motor decline and decreases SOD1 deposition in ALS mice. Experimental Neurology 213:448-455. doi:10.1016/j.expneurol.2008.07.017

13. Kim DI, Jensen SC, Noble KA, Kc B, Roux KH, Motamedchaboki K, Roux KJ (2016) An improved smaller biotin ligase for BioID proximity labeling. Molecular biology of the cell 27:1188-1196. doi:10.1091/mbc.E15-12-0844

14. Kim DI, Roux KJ (2016) Filling the Void: Proximity-Based Labeling of Proteins in Living Cells. Trends in Cell Biology 26:804-817. doi:10.1016/j.tcb.2016.09.004

15. Kim HJ, Kim NC, Wang Y-D, Scarborough EA, Moore J, Diaz Z, Maclea KS, Freibaum B, Li S, Molliex A, Kanagaraj AP, Carter R, Boylan KB, Wojtas AM, Rademakers R, Pinkus JL, Greenberg SA, Trojanowski JQ, Traynor BJ, Smith BN (2013) Mutations in prion-like domains in hnRNPA2B1 and hnRNPA1 cause multisystem proteinopathy and ALS.

16. Kurzban GP, Bayer EA, Wilchek M, Horowitz PM (1991) The quaternary structure of streptavidin in urea. The Journal of biological chemistry 266:14470-14477

17. Laird FM, Farah MH, Ackerley S, Hoke A, Maragakis N, Rothstein JD, Griffin J, Price DL, Martin LJ, Wong PC (2008) Motor neuron disease occurring in a mutant dynactin mouse model is characterized by defects in vesicular trafficking. The Journal of neuroscience : the official journal of the Society for Neuroscience 28:1997-2005. doi:10.1523/JNEUROSCI.4231-

18. Lam SS, Martell JM, Kramer KJ, Deerinck TJ, Ellisman MH, Mootha VK, Ting AY (2014) Directed evolution of APEX2 for electron microscopy and proximity labeling. Nature methods. doi:10.1038/nmeth.3179

19. Lee A, Rayner S, Gwee S, Luca A, Shahheydari H, Sundaramoorthy V, Ragagnin A, Morsch M, Radford R, Galper J, Freckleton S, Shi B, Walker A, Don E, Cole N, Yang S, Williams K, Yerbury J, Blair I, Atkin J, Molloy M, Chung R (2018) Pathogenic mutation in the ALS/FTD gene, CCNF, causes elevated Lys48-linked ubiquitylation and defective autophagy. Cellular and Molecular Life Sciences 75:335-354. doi:10.1007/s00018-017-2632-8

20. Lee C (2007) Protein extraction from mammalian tissues. Methods in molecular biology (Clifton, NJ) 362:385

21. Ling S-C, Polymenidou M, Cleveland DW (2013) Converging Mechanisms in ALS and FTD: Disrupted RNA and Protein Homeostasis. Neuron 79:416-438. doi:10.1016/j.neuron.2013.07.033

22. Malik AM, Miguez RA, Li X, Ho Y-S, Feldman EL, Barmada SJ (2018) Matrin 3-dependent neurotoxicity is modified by nucleic acid binding and nucleocytoplasmic localization. eLife 7. doi:10.7554/eLife.35977

23. Ngounou Wetie AG, Sokolowska I, Woods AG, Roy U, Loo JA, Darie CC (2013) Investigation of stable and transient protein-protein interactions: Past, present, and future. vol 13. doi:10.1002/pmic.201200328 ⌑

24. Okada M, Yamashita S, Ueyama H, Ishizaki M, Maeda Y, Ando Y (2018) Long-term effects of edaravone on survival of patients with amyotrophic lateral sclerosis. eNeurologicalSci 11:11-14. doi:10.1016/j.ensci.2018.05.001

25. Rhee H-W, Zou P, Udeshi ND, Martell JD, Mootha VK, Carr SA, Ting AY (2013) Proteomic mapping of mitochondria in living cells via spatially restricted enzymatic tagging. Science (New York, NY) 339:1328-1331. doi:10.1126/science.1230593

26. Riviere M, Meininger V, Zeisser P, Munsat T (1998) An Analysis of Extended Survival in Patients With Amyotrophic Lateral Sclerosis Treated With Riluzole. Archives of Neurology 55:526-528. doi:10.1001/archneur.55.4.526

27. Roux KJ, Kim DI, Burke B (2013) BioID: A Screen for Protein-Protein Interactions. Current Protocols in Protein Science 74:19.23.11-19.23.14. doi:10.1002/0471140864.ps1923s74

28. Roux KJ, Kim DI, Raida M, Burke B (2012) A promiscuous biotin ligase fusion protein identifies proximal and interacting proteins in mammalian cells. The Journal of cell biology 196:801-810. doi:10.1083/jcb.201112098

29. Ruegsegger Cl, Saxena S (2016) Proteostasis impairment in ALS. Brain Research 1648:571-579. doi:10.1016/j.brainres.2016.03.032

30. Salton M, Lerenthal Y, Wang S-Y, Chen DJ, Shiloh Y (2010) Involvement of Matrin 3 and SFPQ/NONO in the DNA damage response. Cell Cycle 9:1568-1576. doi:10.4161/cc.9.8.11298

31. Sano T, Vajda S, Cantor CR (1998) Genetic engineering of streptavidin, a versatile affinity tag. Journal of chromatography B, Biomedical sciences and applications 715:85-91

32. Scotter E, Chen H-J, Shaw C (2015) TDP-43 Proteinopathy and ALS: Insights into Disease Mechanisms and Therapeutic Targets. The Journal of the American Society for Experimental NeuroTherapeutics 12:352-363. doi:10.1007/s13311-015-0338-x

33. Sundaramoorthy V, Walker AK, Tan V, Fifita JA, McCann EP, Williams KL, Blair IP, Guillemin GJ, Farg MA, Atkin JD (2015) Defects in optineurin- and myosin VI-

mediated cellular trafficking in amyotrophic lateral sclerosis. Human molecular genetics 24:3830-3846. doi:10.1093/hmg/ddv126

34. Weihui, Huang, Dawei, Zang, Yi, Lu, Ping, Jiang (2012) Basic fibroblast growth factor increases the numbe of endogenous neural stem cells and inhibits the expression of amino methyl isoxazole propionic acid receptors in amyotrophic lateral sclerosis mice - Basic fibroblast growth factor increases the number of endogenous neural stem cells and inhibits the expression of amino methyl isoxazole propionic acid receptors in amyotrophic lateral sclerosis mice. Neural Regeneration Research 7:761-765. doi:10.3969/j.issn.1673-5374.2012.10.007

35. Williams KL, Topp S, Yang S, Smith B, Fifita JA, Warraich ST, Zhang KY, Farrawell N, Vance C, Hu X, Chesi A, Leblond CS, Lee A, Rayner SL, Sundaramoorthy V, Dobson-Stone C, Molloy MP, van Blitterswijk M, Dickson DW, Petersen RC, Graff-Radford NR, Boeve BF, Murray ME, Pottier C, Don E, Winnick C, McCann EP, Hogan A, Daoud H, Levert A, Dion PA, Mitsui J, Ishiura H, Takahashi Y, Goto J, Kost J, Gellera C, Gkazi AS, Miller J, Stockton J, Brooks WS, Boundy K, Polak M, Munoz-Blanco JL, Esteban-Perez J, Rabano A, Hardiman O, Morrison KE, Ticozzi N, Silani V, de Belleroche J, Glass JD, Kwok JB, Guillemin GJ, Chung RS, Tsuji S, Brown RH, Jr., Garcia-Redondo A, Rademakers R, Landers JE, Gitler AD, Rouleau GA, Cole NJ, Yerbury JJ, Atkin JD, Shaw CE, Nicholson GA, Blair IP (2016) CCNF mutations in amyotrophic lateral sclerosis and frontotemporal dementia. Nature communications 7:11253. doi:10.1038/ncomms11253

36. Yang S, Zhang KY, Kariawasam R, Bax M, Fifita JA, Ooi L, Yerbury JJ, Nicholson GA, Blair IP (2015) Evaluation of skin fibroblasts from amyotrophic lateral sclerosis patients for the rapid study of pathological features. Springer. doi:10.1007/s12640-015-9532-1
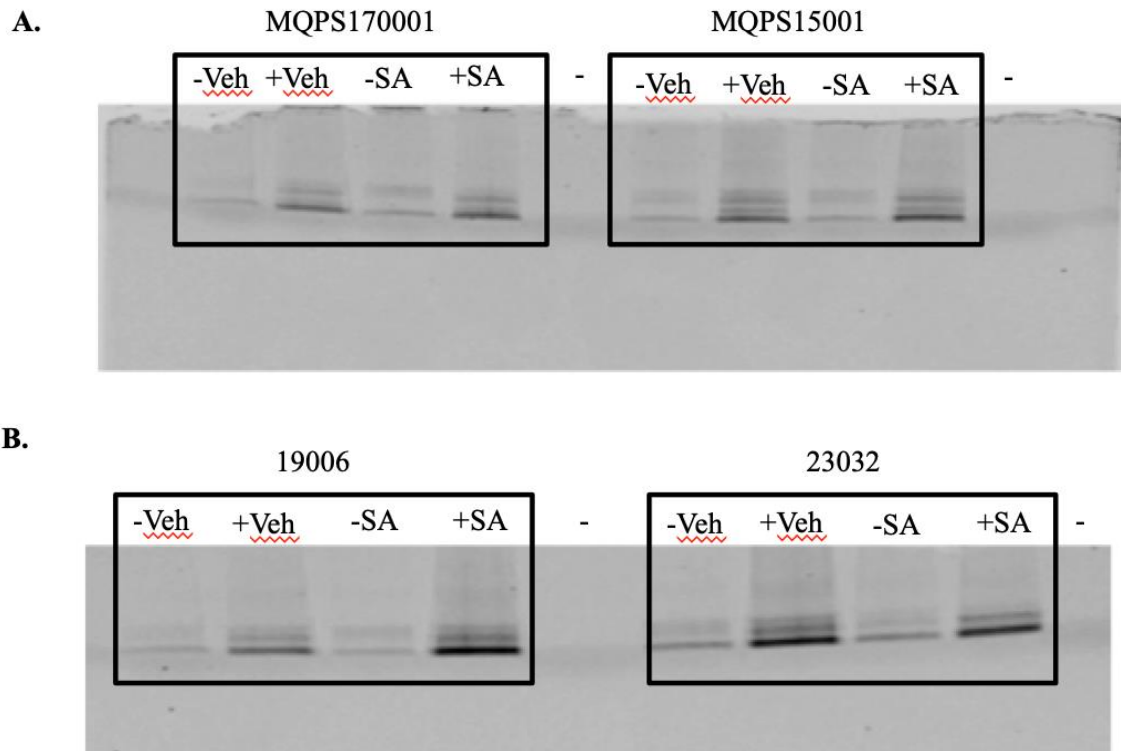
Supplementary material

Fig S1 Images of MS gels containing fibroblast samples with (+) and without (-) primary antibody. Images taken with LiCor Odyssey CLx. **A.** Gel of WT samples MQPS170001 and MQPS15001. **B.** Gel of S621G carrier (19006) and S621G ALS patient (23032). Blank wells are labeled with (-).

CHAPTER 5   Discussion and Future Directions

5.1 Discussion

In this proof-of-concept study, we were able to demonstrate the efficacy of BAR labeling as an unbiased approach to studying pathological inclusions in neurodegenerative diseases. The labeling worked well in both the fixed tissue and cultured fibroblasts with many known disease-related proteins being identified using the BAR-MS workflow. There are, however, a few obstacles to overcome to further develop this method in both the tissue and fibroblast studies with many questions coming up still needing answers. Furthermore, due to the impact of COVID-19, many planned experiments and more in-depth data analysis were not feasible and will be conducted over the next few months prior to submission of articles.

5.1.1 Postmortem tissue considerations

Some major point of consideration when working with BAR for aggregate studies is the tissue quality, antibody quality and how prevalent the aggregates are. Tissue with a high amount of inclusions would provide more insight into their composition, as the data would be more robust and could therefore provide reliable results to draw significant conclusions. Additionally, a quality primary antibody is crucial for specific binding to the target of interest to obtain data that are more accurate [3]. This point is further described in future directions. This brought up another issue within the process of isolating proteins and preparing them for analyses. Due to variability in overall protein concentration, between 120μg and 200μg of protein lysate in BAR lysis buffer was used for the pull-down for PSP tissue experiments. This meant there was less consistency across the samples, and many proteins (especially low abundance proteins) may have been missed due to this and a variety of other reasons that are covered in future directions.

5.1.2 Understanding stress-induced TDP-43 pathology in fibroblasts

A goal of the second half of the project was to understand under what conditions would fibroblasts show TDP-43 pathology. We found that 500μM SA provided the best results for overall TDP-43 compared to MG132, so this was used for the rest of the project. After the proteins were isolated and identified with MS, the datasets were compared between the samples. The first question we asked is if WT fibroblasts develop TDP-43 pathology with SA treatment. Through IPA analysis, TDP-43 is not in the SA treated sample, but rather completely in the vehicle control (-100 AR). With comparative IHC under the confocal microscope, it was observed that mutant S621G cells have much more TDP-43 showing up

82

than WT cells when treated with SA and the vehicle control. This led to the next question, to see if the S621G mutation itself causes increased TDP-43 pathology compared to WT, just the vehicle controls for both conditions were compared against each other. The data illustrates a 4.687 fold change in TDP-43 in the mutant control compared to WT control, which alludes to the fact that the hypothesis may be true. Then, the SA treated S621G and SA treated WT were compared to see how much the cell stressor treatment of SA increased TDP-43 pathology. We found that TDP-43 was increased by 100-fold in the mutant (S621G) sample suggesting that both the ALS mutation and the stressor combined result in high TDP-43 in the cell. Further, we asked how the S621G cells treated with SA compare to a S621G vehicle control. Interestingly, TDP-43 was found to be at a -2.141 fold change, meaning the vehicle control has more TDP-43 here. This contradicts what is observed on the confocal images comparing the conditions. However, mass cell death was typically observed in SA treated cells, which may account for a lower amount of TDP-43 due to a slightly lower density of cells. Another reason for this may be that we have only studied the soluble fraction and it is known that TDP-43 aggregates in ALS are insoluble and so TDP-43 may remain in the insoluble fraction of the S621G SA sample that had not yet been studied. This will need to be investigated further and optimized in future experiments. Nevertheless, the data shows TDP-43 levels are still much higher in the S621G SA treated sample compared to the WT SA treated samples.

5.1.3 IPA and functional analysis

IPA is an excellent tool to quickly analyze and categorize large protein datasets. In this thesis, all datasets were analysed with the protein abundance threshold set at >1.5 fold change and the Bioprofiler function was used to categorize these proteins further into being involved in tauopathies and PSP, or ALS, as well as neurodegeneration. Although this came up with many proteins, some proteins such as heat shock proteins [40], 14-3-3 family proteins [2], and RNA-binding proteins [16] did not appear although they are in the raw datasets. Many times, these proteins were in low abundance, not meeting the AR threshold, and therefore did not show in IPA at all, however many samples did show these proteins with an AR of >1.5. This is a significant limitation found in IPA as data analysis still requires a fair amount of manual analysis. Addressing and rectifying this problem is a goal over the next few months to get the most out of the data using IPA software.

5.2 Future Directions

5.2.1 Antibodies illustrate pathology at various stages of disease

BAR relies on high quality and precise antibodies that label the protein of interest and reduce non-specific binding [3]. There is a large volume of antibodies to chose from and attach to different parts of the protein or different forms of the protein. Here it was shown that the tau antibody used (AT180) bonded to tau in its mature stage of PSP pathology, whereas the AT8 antibody binds to tau of all stages of pathology. A comparison between these, and other, tau antibodies may elucidate the differences between different stages of pathology providing insight into the disease mechanisms at play from early stage to end stage of the disease. Moreover, this will be taken into consideration with TDP-43 antibodies that label all TDP-43 versus pathological TDP-43. With this, we can do a statistical analysis of how much TDP-43 pathology there is in each imaged sample, and compare this to the proteomic analysis conducted later. Additionally, it would be beneficial to study tau pathology across various diseases and identify the similarities and differences in how tau acts between diseases. In particular, sections of post-mortem brain tissue from patients that were afflicted with Alzheimer's Disease are available for the Chung lab to use and will be compared to the findings of tau pathology in PSP. The same concept can be applied to TDP-43 pathology in ALS and frontotemporal dementia using cultured fibroblasts and postmortem brain sections of ALS patients recently collected in our lab.

5.2.2 Overcoming the challenge of insoluble proteins

A major hallmark of neurodegenerative pathologies is that of insoluble aggregates forming within neurons. These insoluble fractions require additional steps to be solubilized for study. Solubilizing these aggregates for study is difficult and may result in sample loss however it is important to still look into the insoluble fractions to identify any important proteins that form p-Tau and TDP-43 aggregates. It is expected that the major aggregating proteins are left in the insoluble fraction and hence do not appear in the raw data as very abundant. The amount of protein that does show up may be regular soluble protein that is typically inside their respective cells, whether healthy or diseased. Therefore, a sequential extraction will be performed to isolate soluble then insoluble proteins from each sample.

5.2.3 How a pre-symptomatic carrier of an ALS mutation can provide insight into the beginning stages of disease formation

Although important to look at the healthy and pathological interactomes of aggregates within fibroblasts, it would be an interesting comparison to also analyse the interactome of a pre-symptomatic case of ALS with the S621G mutation. In theory, a pre-symptomatic carrier should have an interactome comparable to that of a healthy patient. However, this may not necessarily be the case and can start to resemble a pathological interactome. This can be used to distinguish different stages of diseases and to unravel the pathogenesis of TDP-43 aggregation in ALS from upstream effects, which can reveal the mechanisms at play at different stages of disease that can then be targeted therapeutically. The same workflow explained in article II will be employed along with proteomic validation explained in section 5.2.4. Additionally, it would be interesting to compare the interactome of a variety of patients with different ALS-causing mutations (e.g. *SOD1* mutations, *C9orf72* variants, as well as other variants) to understand the differences and similarities are between them, adding it to the big picture and hopefully finding a therapeutic target that works for most, if not all, cases. In addition, the mutations for each patient will be validated using polymerase chain reaction and next generation sequencing.

5.2.4 Validation of protein interactome data

To validate the findings of known and potential co-aggregators of p-Tau and TDP-43, standard IHC and co-immunoprecipitation will be conducted. Additionally, to address the limitation of sample amount, fibroblasts will be grown in multiple larger flasks and repeat experiments will be conducted for more robust and reliable data. Although this comes with concern surrounding antibody cost, this section of the protocol will be further optimized to limit the amount of primary antibody needed to appropriately label TDP-43. Furthermore, the BAR method will be compared to the conventional biochemical extraction method with MS for protein identification to see how the results differ, with subsequent validation using the techniques described above. This is to maintain consistent methodology and not relying on papers, as protocols may differ and therefore produce varying results. Lastly, it would be important to conduct statistical analysis of fibroblast images using Imaris to identify how much TDP-43 is found within the nucleus and how much TDP-43 has mislocalized to the cytoplasm. Doing so would provide a better understanding of the data that comes from the MS and if aggregates are actually forming.

5.2.5 Optimization

Although the method had been optimized early in the project, after analysing the results and reviewing the limitations, it would be a good idea to optimize some protocols further to ensure clean results. Some considerations for optimization include biotin cleavage and fibroblast drug treatments.

As many of the proteins thought to be more abundant (i.e. p-Tau and TDP-43) showed low abundance in the data not meeting the AR threshold, it could be worthwhile to revisit the streptavidin beads used for this study that were saved and left in the -80°C freezer. Here, we will try to cleave off any proteins still attached to the beads and analyse what proteins appear after MS protein identification. If it appears that many crucial proteins remained on the beads, this protocol will need to be optimized with DTT concentration and boiling of the beads, as the boiling process has been used by SR and RR with their use of biotin-XX-tyramide to remove all the proteins from the beads. If this does not yield any extra protein, then the insoluble fractions would be more useful to study, as described in section 5.2.2.

Although the study showed an observable increase of TDP-43 in SA treated fibroblasts and the data presented proteins involved in ALS, neurodegeneration and the stress response, there have been limitations to the drug treatment protocol that need to be addressed. In particular, we want to create more pathology within the cells while minimizing cell death associated with SA exposure. A starting point is to lower the concentration of SA and leave it on for a longer period, observe what happens, and then reassess.

5.3 Conclusion and significance

Overall, the BAR-MS approach taken in this project has shed some light onto potential novel proteins and mechanisms that play a role in PSP and ALS aggregate formation, along with proteins known to be involved in these diseases. Future validation of the above findings and repeated experiments will show some conclusive insight into the interactome of p-Tau and TDP-43 aggregates described here. Identification of the molecular composition of aggregates will lead to targeted therapeutic approaches for formation prevention and findings of common biomarkers that are cell specific may become clinical diagnostic tools in early stages, rather than validation on postmortem examination. This proof-of-concept study

reveals that there is a lot of potential for the BAR-MS approach with broad research applications, allowing this study to be taken to the next stage as described above.

References

1. Arai T, Nonaka T, Hasegawa M, Akiyama H, Yoshida M, Hashizume Y, Tsuchiya K, Oda T, Ikeda K (2003) Neuronal and glial inclusions in frontotemporal dementia with or without motor neuron disease are immunopositive for p62. Neuroscience Letters 342:41-44. doi:10.1016/S0304-3940(03)00216-7

2. Arendt T, Stieler JT, Holzer M (2016) Tau and tauopathies. Brain Research Bulletin 126:238-292. doi:10.1016/j.brainresbull.2016.08.018

3. Bar DZ, Atkatsh K, Tavarez U, Erdos MR, Gruenbaum Y, Collins FS (2017) Biotinylation by antibody recognition: a method for proximity labeling. Nature methods 15. doi:10.1038/nmeth.4533

4. Beere HM (2004) "The stress of dying": the role of heat shock proteins in the regulation of apoptosis. Journal of cell science 117:2641. doi:10.1242/jcs.01284

5. Blokhuis A, Groen E, Koppers M, Berg L, Pasterkamp R (2013) Protein aggregation in amyotrophic lateral sclerosis. Pathology and Mechanisms of Neurological Disease 125:777-794. doi:10.1007/s00401-013-1125-6

6. Chen C-L, Perrimon N (2017) Proximity-dependent labeling methods for proteomic profiling in living cells. Wiley Interdisciplinary Reviews 6. doi:10.1002/wdev.272

7. Cho JH, Hwang HY, Cho MH, Kwon YK, Jeon JS, Bhoo SHE, Hahn TRE (2008) The effect of DTT in protein preparations for proteomic analysis: Removal of a highly abundant plant enzyme, ribulose bisphosphate carboxylase/oxygenase. Journal of Plant Biology 51:297-301. doi:10.1007/BF03036130

8. Coffey CM, Gronert S (2016) A cleavable biotin tagging reagent that enables the enrichment and identification of carbonylation sites in proteins. Analytical and bioanalytical chemistry 408:865. doi:10.1007/s00216-015-9176-2

9. Cuatrecasas P, Wilchek M, Anfinsen CB (1968) Selective Enzyme Purification by Affinity Chromatography. Proceedings of the National Academy of Sciences of the United States of America 61:636-643. doi:10.1073/pnas.61.2.636

10. Fang T, Al Khleifat A, Meurgey J-H, Jones A, Leigh PN, Bensimon G, Al-Chalabi A (2018) Stage at which riluzole treatment prolongs survival in patients with amyotrophic lateral sclerosis: a retrospective analysis of data from a dose-ranging study. The Lancet Neurology 17:416-422.

11. Flynn JM, Melov S (2013) SOD2 in mitochondrial dysfunction and neurodegeneration. Free Radical Biology and Medicine 62:4-12.

doi:10.1016/j.freeradbiomed.2013.05.027

12. Fredriksson S, Gullberg M, Jarvius J, Olsson C, Pietras K, Gústafsdóttir SM, Östman A, Ulf L (2002) Protein detection using proximity-dependent DNA ligation assays. Nature biotechnology 20:473. doi:10.1038/nbt0502-473

13. Golbe LI (2014) Progressive supranuclear palsy. Seminars in neurology 34:151-159. doi:10.1055/s-0034-1381736

14. Green, NM (1990) Avidin and streptavidin. Methods Enzymol. 184, 51–67.

15. Guil S, Long JC, Caceres JF (2006) hnRNP A1 Relocalization to the Stress Granules Reflects a Role in the Stress Response. Molecular and Cellular Biology 26:5744. doi:10.1128/MCB.00224-06

16. Heemels M-T. (2016) Neurodegenerative diseases. Nature 539:179. doi:10.1038/539179a

17. Huang C-C, Bose JK, Majumder P, Lee K-H, Huang J-TJ, Huang JK, Shen C-KJ (2014) Metabolism and mis-metabolism of the neuropathological signature protein TDP-43. Journal of cell science 127:3024-3038. doi:10.1242/jcs.136150

18. Hughes D, Mallucci GR (2019) The unfolded protein response in neurodegenerative disorders - therapeutic modulation of the PERK pathway. FEBS Journal 286:342. doi:10.1111/febs.14422

19. Ito H, Wate R, Zhang J, Ohnishi S, Kaneko S, Ito H, Nakano S, Kusaka H (2008) Treatment with edaravone, initiated at symptom onset, slows motor decline and decreases SOD1 deposition in ALS mice. Experimental Neurology 213:448-455. doi:10.1016/j.expneurol.2008.07.017

20. Jadhav S, Avila J, Scholl M, Kovacs GG, Kovari E, Skrabana R, Evans LD, Kontsekova E, Malawska B, de Silva R, Buee L, Zilka N (2019) A walk through tau therapeutic strategies. Acta Neuropathologica Communications 7. doi:10.1186/s40478-019-0664-z

21. Johnson JO, Mandrioli J, Benatar M, Abramzon Y, Van Deerlin VM, Trojanowski JQ, Gibbs JR, Brunetti M, Gronka S, Wuu J, Ding J, McCluskey L, Martinez-Lage M, Falcone D, Hernandez DG, Arepalli S, Chong S, Schymick JC, Rothstein J, Landi F (2011) Exome Sequencing Reveals VCP Mutations as a Cause of Familial ALS. Neuron 69:397-397. doi:10.1016/j.neuron.2011.01.009

22. Kim DI, Jensen SC, Noble KA, Kc B, Roux KH, Motamedchaboki K, Roux KJ (2016) An improved smaller biotin ligase for BioID proximity labeling. Molecular biology of the cell 27:1188-1196. doi:10.1091/mbc.E15-12-0844

23. Kim DI, Roux KJ (2016) Filling the Void: Proximity-Based Labeling of Proteins in Living Cells. Trends in Cell Biology 26:804-817. doi:10.1016/j.tcb.2016.09.004

24. Kurepa J, Walker JM, Smalle J, Gosink MM, Davis SJ, Durham TL, Sung D-Y, Vierstra RD (2003) The small ubiquitin-like modifier (SUMO) protein modification system in Arabidopsis. Accumulation of SUMO1 and -2 conjugates is increased by stress. The Journal of biological chemistry 278:6862-6872. doi:10.1074/jbc.M209694200

25. Kurzban GP, Bayer EA, Wilchek M, Horowitz PM (1991) The quaternary structure of streptavidin in urea. The Journal of biological chemistry 266:14470-14477

26. Lam SS, Martell JM, Kramer KJ, Deerinck TJ, Ellisman MH, Mootha VK, Ting AY (2014) Directed evolution of APEX2 for electron microscopy and proximity labeling. Nature methods. doi:10.1038/nmeth.3179

27. Lattante S, de Calbiac H, Le Ber I, Brice A, Ciura S, Kabashi E (2015) Sqstm1 knock-down causes a locomotor phenotype ameliorated by rapamycin in a zebrafish model of ALS/FTLD. Human molecular genetics 24:1682-1690. doi:10.1093/hmg/ddu580

28. Lee C (2007) Protein extraction from mammalian tissues. Methods in molecular biology (Clifton, NJ) 362:385

29. Lee A, Rayner S, Gwee S, Luca A, Shahheydari H, Sundaramoorthy V, Ragagnin A, Morsch M, Radford R, Galper J, Freckleton S, Shi B, Walker A, Don E, Cole N, Yang S, Williams K, Yerbury J, Blair I, Atkin J, Molloy M, Chung R (2018) Pathogenic mutation in the ALS/FTD gene, CCNF, causes elevated Lys48-linked ubiquitylation and defective autophagy. Cellular and Molecular Life Sciences 75:335-354. doi:10.1007/s00018-017-2632-8

30. Li W, Zeng W, Chen Y, Wang F, Wu F, Weng X, Zhou X (2019) Biotinylation and isolation of an RNA G-quadruplex based on its peroxidase-mimicking activity. Analyst 144:4472-4476. doi:10.1039/c9an00353c

31. Ling S-C, Polymenidou M, Cleveland DW (2013) Converging Mechanisms in ALS and FTD: Disrupted RNA and Protein Homeostasis. Neuron 79:416-438. doi:10.1016/j.neuron.2013.07.033

32. Maruyama H, Morino H, Ito H, Izumi Y, Kato H, Watanabe Y, Kinoshita Y, Kamada M, Nodera H, Suzuki H, Komure O, Mat- suura S, Kobatake K, Morimoto N, Abe K, Suzuki N, Aoki M, Kawata A, Hirai T, Kato T, Ogasawara K, Hirano A, Takumi T, Kusaka H, Hagiwara K, Kaji R, Kawakami H (2010) Mutations of optineurin in

amyotrophic lateral sclerosis. Nature 465:223. doi:10.1038/nature08971

33. Miller BL (2013) The C9ORF72 mutation brings more answers and more questions. Alzheimer's research & therapy 5:7-7. doi:10.1186/alzrt161

34. Munch DC, Sedlmeier OR, Meyer CT, Homberg CV, Sperfeld CA, Kurt CA, Prudlo CJ, Peraus CG, Hanemann CC, Stumm CG, Ludolph CA (2004) Point mutations of the p150 subunit of dynactin (DCTN1) gene in ALS. Neurology 63:724-726. doi:10.1212/01.WNL.0000134608.83927.B1

35. Nassif M, Valenzuela V, Rojas-Rivera D, Vidal R, Matus S, Castillo K, Fuentealba Y, Kroemer G, Levine B, Hetz C (2014) Pathogenic role of BECN1/Beclin 1 in the development of amyotrophic lateral sclerosis. Autophagy 10:1256-1271. doi:10.4161/auto.28784

36. National Institute of Neurological Disorders and Stroke (2020) Progressive Supranuclear Palsy Fact Sheet. NINDS. https://www.ninds.nih.gov/Disorders/Patient-Caregiver-Education/Fact-Sheets/Progressive-Supranuclear-Palsy-Fact-Sheet

37. Ngounou Wetie AG, Sokolowska I, Woods AG, Roy U, Loo JA, Darie CC (2013) Investigation of stable and transient protein-protein interactions: Past, present, and future. vol 13. doi:10.1002/pmic.201200328

38. Okada M, Yamashita S, Ueyama H, Ishizaki M, Maeda Y, Ando Y (2018) Long-term effects of edaravone on survival of patients with amyotrophic lateral sclerosis. eNeurologicalSci 11:11-14. doi:10.1016/j.ensci.2018.05.001

39. Pankiv S, Clausen TH, Lamark T, Brech A, Bruun J-A, Outzen H, Øvervatn A, Bjørkøy G, Johansen T (2007) p62/SQSTM1 binds directly to Atg8/LC3 to facilitate degradation of ubiquitinated protein aggregates by autophagy. The Journal of biological chemistry 282:24131-24145. doi:10.1074/jbc.M702824200

40. Priya S, Sharma SK, Goloubinoff P (2013) Molecular chaperones as enzymes that catalytically unfold misfolded polypeptides. vol 587. doi:10.1016/j.febslet.2013.05.014

41. Puls I, Jonnakuty C, LaMonte BH, Holzbaur EL, Tokito M, Mann E, Floeter MK, Bidus K, Drayna D, Oh SJ, Brown RH Jr., Lud- low CL, Fischbeck KH (2003) Mutant dynactin in motor neuron disease. Nature Genetics 33:455. doi:10.1038/ng1123

42. Renton AE, Chiò A, Traynor BJ (2014) State of play in amyotrophic lateral sclerosis genetics. Nature neuroscience 17:17. doi:10.1038/nn.3584

43. Rhee H-W, Zou P, Udeshi ND, Martell JD, Mootha VK, Carr SA, Ting AY (2013)

Proteomic mapping of mitochondria in living cells via spatially restricted enzymatic tagging. Science (New York, NY) 339:1328-1331. doi:10.1126/science.1230593

44. Richardson JC, Steele J, Olszewski J (1963) Supranuclear ophthalmoplegia, pseudobulbar palsy, nuchal dystonia and dementia. A clinical report on eight cases of "heterogenous system degeneration". Transactions of the American Neurological Association 88:25-29

45. Riviere M, Meininger V, Zeisser P, Munsat T (1998) An Analysis of Extended Survival in Patients With Amyotrophic Lateral Sclerosis Treated With Riluzole. Archives of Neurology 55:526-528. doi:10.1001/archneur.55.4.526

46. Roux KJ, Kim DI, Burke B (2013) BioID: A Screen for Protein-Protein Interactions. Current Protocols in Protein Science 74:19.23.11-19.23.14. doi:10.1002/0471140864.ps1923s74

47. Roux KJ, Kim DI, Raida M, Burke B (2012) A promiscuous biotin ligase fusion protein identifies proximal and interacting proteins in mammalian cells. The Journal of cell biology 196:801-810. doi:10.1083/jcb.201112098

48. Ruegsegger Cl, Saxena S (2016) Proteostasis impairment in ALS. Brain Research 1648:571-579. doi:10.1016/j.brainres.2016.03.032

49. Sano T, Vajda S, Cantor CR (1998) Genetic engineering of streptavidin, a versatile affinity tag. Journal of chromatography B, Biomedical sciences and applications 715:85-91

50. Schraen-Maschke S, Sergeant N, Dhaenens C-M, Bombois Sp, Deramecourt V, Caillet-Boudin M-L, Pasquier F, Maurage C-A, Sablonnière B, Vanmechelen E, Buée L (2008) Tau as a biomarker of neurodegenerative diseases. Biomarkers in medicine 2:363-384. doi:10.2217/17520363.2.4.363

51. Scotter E, Chen H-J, Shaw C (2015) TDP-43 Proteinopathy and ALS: Insights into Disease Mechanisms and Therapeutic Targets. The Journal of the American Society for Experimental NeuroTherapeutics 12:352-363. doi:10.1007/s13311-015-0338-x

52. Scotter EL, Vance C, Nishimura AL, Lee Y-B, Chen H-J, Urwin H, Sardone V, Mitchell JC, Rogelj B, Rubinsztein DC, Shaw CE (2014) Differential roles of the ubiquitin proteasome system and autophagy in the clearance of soluble and aggregated TDP-43 species. Journal of cell science 127:1263-1278. doi:10.1242/jcs.140087

53. Sergeant N, Bretteville A, Hamdane M, Caillet-Boudin M-L, Grognet P, Bombois S, Blum D, Delacourte A, Pasquier F, Vanmechelen E, Schraen-Maschke S, Buée L

(2008) Biochemistry of Tau in Alzheimer's disease and related neurological disorders. Expert Review of Proteomics 5:207-224. doi:10.1586/14789450.5.2.207

54.   Shen W-C, Li H-Y, Chen G-C, Chern Y, Tu P-H (2015) Mutations in the ubiquitin-binding domain of OPTN/optineurin interfere with autophagy-mediated degradation of misfolded proteins by a dominant-negative mechanism. Autophagy 11:685-700. doi:10.4161/auto.36098

55.   Sundaramoorthy V, Walker AK, Tan V, Fifita JA, McCann EP, Williams KL, Blair IP, Guillemin GJ, Farg MA, Atkin JD (2015) Defects in optineurin- and myosin VI-mediated cellular trafficking in amyotrophic lateral sclerosis. Human molecular genetics 24:3830-3846. doi:10.1093/hmg/ddv126

56.   Wang IF, Tsai K-J, Shen C-KJ (2013) Autophagy activation ameliorates neuronal pathogenesis of FTLD-U mice: A new light for treatment of TARDBP/TDP-43 proteinopathies. Autophagy 9:239-240. doi:10.4161/auto.22526

57.   Wijesekera LC Leigh PN, (2009) Amyotrophic lateral sclerosis. Orphanet Journal of Rare Diseases 4:3. doi:10.1186/1750-1172-4-3

58.   Williams KL, Topp S, Yang S, Smith B, Fifita JA, Warraich ST, Zhang KY, Farrawell N, Vance C, Hu X, Chesi A, Leblond CS, Lee A, Rayner SL, Sundaramoorthy V, Dobson-Stone C, Molloy MP, van Blitterswijk M, Dickson DW, Petersen RC, Graff-Radford NR, Boeve BF, Murray ME, Pottier C, Don E, Winnick C, McCann EP, Hogan A, Daoud H, Levert A, Dion PA, Mitsui J, Ishiura H, Takahashi Y, Goto J, Kost J, Gellera C, Gkazi AS, Miller J, Stockton J, Brooks WS, Boundy K, Polak M, Munoz-Blanco JL, Esteban-Perez J, Rabano A, Hardiman O, Morrison KE, Ticozzi N, Silani V, de Belleroche J, Glass JD, Kwok JB, Guillemin GJ, Chung RS, Tsuji S, Brown RH, Jr., Garcia-Redondo A, Rademakers R, Landers JE, Gitler AD, Rouleau GA, Cole NJ, Yerbury JJ, Atkin JD, Shaw CE, Nicholson GA, Blair IP (2016) CCNF mutations in amyotrophic lateral sclerosis and frontotemporal dementia. Nature communications 7:11253. doi:10.1038/ncomms11253

59.   Yang S, Zhang KY, Kariawasam R, Bax M, Fifita JA, Ooi L, Yerbury JJ, Nicholson GA, Blair IP (2015) Evaluation of skin fibroblasts from amyotrophic lateral sclerosis patients for the rapid study of pathological features. Springer. doi:10.1007/s12640-015-9532-1

MACQUARIE
University
SYDNEY·AUSTRALIA

30 June 2016

Dear Associate Professor Blair

Reference No: 5201600387

Title: *Macquarie University Neurodegenerative Disease Biobank*

Thank you for submitting the above application for ethical and scientific review. Your application was considered by the Macquarie University Human Research Ethics Committee (HREC (Medical Sciences)).

I am pleased to advise that ethical and scientific approval has been granted for this project to be conducted at:

- Macquarie University

This approval is subject to the following conditions as determined by the HREC (Medical Sciences) Executive:

- For Macquarie University Researchers (internal) accessing samples from the Biobank to conduct research that fits within the scope of current HREC approval, approval will be sought from the Biobank Committee. The Biobank committee will provide quarterly reports to the HREC on the research being conducted using the samples and the investigators involved.

- For Macquarie University Researchers (internal) accessing samples from the Biobank to conduct research that does not fit within the scope of current HREC approval, ethics approval must be sought from the MDS HREC.

- For External researchers wishing to access samples from the Biobank, Biobank approval will be sought. The Biobank committee will provide the MDS HREC with:

    o Information on the research being conducted using the samples

    o An MTA covering transfer of samples

    o A copy of the external institutions ethics application and ethics approval covering use of samples.

- This will be done for each request made by an external researcher and research will not commence using the samples until approval by the MDS HREC has been finalised.

This research meets the requirements set out in the *National Statement on Ethical Conduct in Human Research* (2007 – Updated May 2015) (the *National Statement*).

Standard Conditions of Approval:

1. Continuing compliance with the requirements of the *National Statement,* which is available at the following website:

http://www.nhmrc.gov.au/book/national-statement-ethical-conduct-human-research

2. This approval is valid for five (5) years, subject to the submission of annual reports. Please submit your reports on the anniversary of the approval for this protocol.

3. All adverse events, including events which might affect the continued ethical and scientific acceptability of the project, must be reported to the HREC within 72 hours.

4. Proposed changes to the protocol and associated documents must be submitted to the Committee for approval before implementation.

It is the responsibility of the Chief investigator to retain a copy of all documentation related to this project and to forward a copy of this approval letter to all personnel listed on the project.

Should you have any queries regarding your project, please contact the Ethics Secretariat on 9850 4194 or by email ethics.secretariat@mq.edu.au

The HREC (Medical Sciences) Terms of Reference and Standard Operating Procedures are available from the Research Office website at:

http://www.research.mq.edu.au/for/researchers/how_to_obtain_ethics_approval/human_research_ethics

The HREC (Medical Sciences) wishes you every success in your research.

Yours sincerely

Professor Tony Eyers
Chair, Macquarie University Human Research Ethics Committee (Medical Sciences)

This HREC is constituted and operates in accordance with the National Health and Medical Research Council's (NHMRC) *National Statement on Ethical Conduct in Human Research* (2007) and the *CPMP/ICH Note for Guidance on Good Clinical Practice*.

Details of this approval are as follows:

Approval Date: 6 June 2016

The following documentation has been reviewed and approved by the HREC (Medical Sciences):

Documents reviewed	Version no.	Date
Macquarie University Ethics Application Form		Received 11/5/2016
Correspondence responding to the issues raised by the HREC (Medical Sciences)		Received 6/6/2016
MQ Participant Information and Consent Form (PICF) entitled '*Neurodegenerative Disease Biobank*'	1	6/6/2016
MQ Withdrawal of Consent form entitled '*Neurodegenerative Disease Biobank*'	1	11/5/2016
Macquarie University Neurodegenerative Disease Biobank Project Request Form	1	11/5/2016s
Questionnaire – Demographics and Education; Biometrics; Ancestry; Residential History; Smoking; Alcohol; Hormones (women only); Operations; Occupations; Physical Activity; Trauma/injury; Use of Drugs/substances; Family History	1	11/5/2016
List of Researchers	1	17/5/2016

*If the document has no version date listed one will be created for you. Please ensure the footer of these documents are updated to include this version date to ensure ongoing version control.

09/12/2019

Dear Professor Julie Atkin,

 Re:"Generation of genetically modified organisms and cell lines to investigate and modify disorders of the nervous system. " 5974 - 52019597412350

NOTIFICATION OF A NOTIFIABLE LOW RISK DEALING (NLRD)

The above application has been reviewed by the Institutional Biosafety Committee (IBC) and has been approved as an NLRD, effective 09/12/2019.

This approval is subject to the following standard conditions:

- The NLRD is conducted by persons with appropriate training and experience, within a facility certified to either Physical Containment level 1 (PC1) or PC2.

- Work requiring Quarantine Containment level 2 (QC2) does not commence until the facility has been certified

Please note the following standard requirements of approval:

1. Approval will be for a period of 5 years subject to the provision of annual reports. If, at the end of this period the project has been completed, abandoned, discontinued or not commenced for any reason, you are required to submit a Final Report. If you complete the work earlier than you had planned you must submit a Final Report as soon as the work is completed. Please contact the Committee Secretary at biosafety@mq.edu.au for a copy of the annual report.

Reporting: Annual progress reports are required for this project and a **Final Report for this project will be due on: 09/12/2024**

2. If you will be applying for or have applied for internal or external funding for the above project it is your responsibility to provide the Macquarie University's Research Grants Management Assistant with a copy of this email as soon as possible. Internal and External funding agencies will not be informed that you have final approval for your project and funds will not be released until the Research Grants Management Assistant has received a copy of this email.

If you need to provide a hard copy letter of approval to an external organisation as evidence that you have approval, please do not hesitate to contact the Committee Secretary at the address below.

Please retain a copy of this letter as this is your formal notification of final Biosafety approval. Also a copy of record submitted by Macquarie University to the OGTR.

Kind Regards,

Professor Robert Willows

Institutional Biosafety Committee Chair,
Macquarie University Research Office
Level 3, Research Hub, Building C5C East
Macquarie University, NSW 2109 Australia
T: +61 2 9850 4063
E: biosafety@mq.edu.au
W: mq.edu.au/research

Level 3, Research Hub   T: +61 (2) 9850 4063   E: biosafety@mq.edu.au
Building c5c East   mq.edu.au/research
Macquarie University
NSW 2109 Australia

ABN 90 952 801 237 | CRICOS Provider 00002J

Page 1 of 1